

KU ScholarWorks

Ecological applications of remote sensing data in neotropical rainforests

Item Type	Dissertation
Authors	Papeş, Monica
Publisher	University of Kansas
Rights	This item is protected by copyright and unless otherwise specified the copyright of this thesis/dissertation is held by the author.
Download date	2024-08-24 18:16:03
Link to Item	https://hdl.handle.net/1808/5454

ECOLOGICAL APPLICATIONS OF REMOTE SENSING DATA IN NEOTROPICAL
RAINFORESTS

BY

Monica Papes

Submitted to the Department of Ecology and Evolutionary Biology
and the Faculty of the Graduate School of The University of Kansas
in partial fulfillment of the requirements for the degree of
Doctor of Philosophy.

Chairperson

Committee members

Date defended: 21 April 2009

The Dissertation Committee for Monica Papes certifies
that this is the approved version of the following dissertation:

ECOLOGICAL APPLICATIONS OF REMOTE SENSING DATA IN NEOTROPICAL
RAINFORESTS

Chairperson

Committee members

Date approved: _____

ABSTRACT

Understanding species' distributions is a central theme of biodiversity studies. A combination of data derived from moderate and high spectral resolution satellite imagery (vegetation indices and hyperspectral narrow bands, respectively) was used to address questions regarding tree species' distributions, vegetation phenology, and influences on bird seasonal movements in tropical rainforests. Vegetation indices were used in ecological niche modeling to predict movement patterns of a tropical canopy frugivorous bird in Central America: the predicted distributions generally recovered observed non-breeding ranges, but estimated lowland areas for the breeding range, which is restricted to middle elevations. Hyperspectral imagery provided sufficient spectral information to discriminate crowns of five different tree taxa that represent food resources for macaws and peccaries in southeastern Peru. Tree spectra showed significant temporal variation, suggesting that it is possible to study tree phenology remotely. Current and future developments of remote sensing techniques permit regional studies of ecosystem functions and structure.

ACKNOWLEDGEMENTS

A long series of very fortunate events led to my writing these lines here in Lawrence, Kansas. First of all, my parents taught me to be independent early in my life, and encouraged me to pursue my academic interests. My husband Árpi Nyári went one step further and encouraged me to continue my studies outside of Romania, an idea that my parents supported fully, even though it limited our time spent together to a few days a year. Town Peterson's decision to accept me in his excellent lab has changed my academic outlook in a way I never would have imagined as an undergraduate student in Romania. He deserves and has earned my deepest and eternal gratitude. Besides vastly broadening my horizons thanks to continuous support and great collaborations initiated in Town's lab, I also accumulated many great memories that I will cherish for as long as old age will allow remembering them (thank you for making the visit to CDC headquarters in Atlanta possible!). Árpi has been absolutely crucial in pursuing and achieving my dreams, and I am very grateful for all his help and patience in the office and at home. My sincere respect and love for his full support.

My interest in tropical ecology has been sparked by an OTS field course I took with Bob Timm in Costa Rica. I thank him for introducing me to the amazing world of tropical biology. I thank Heather York for her companionship during that course and for her help organizing a follow-up trip to Costa Rica which allowed me

to collect data for my first chapter. I also thank Nuría Roura Pascual for her assistance during that field season and for her much cherished friendship.

I had the great pleasure and fortune to meet George Powell, WWF senior scientist, who found my ideas interesting enough to fund them. Without his financial support I wouldn't have been able to do the research presented in chapters two and three. Also crucial in carrying out those studies were Raúl Tupayachi and Paola Martínéz, two excellent Peruvian botanists and friends who collected plant phenology data. I am very grateful to them for their enthusiastic collaboration and friendship. I thank Greg Asner for his excellent review of my second chapter while doing fieldwork together in Peru. His comments and ideas have greatly improved my work. I also thank James Jacobson and Andrew Dyk for their assistance in processing hyperspectral imagery.

For help with statistical questions I thank Norm Slade, Sean Maher, Matt Davis, and Alberto Jimenéz Valverde. I also thank Jorge Soberon, Mark Robbins, and Rob Moyle for discussions and useful comments during my graduate training. I am grateful to my committee members, Ed Wiley, Kirsten Jensen, Ford Ballantyne, and Xingong Li, for providing helpful feedback. Special thanks to Ed Wiley for his continuous and kind encouragements. Many thanks to KU Natural History Museum and Department of Ecology and Evolutionary Biology for logistic and financial support.

My friends in Lawrence have provided the distractions necessary to keep sane and in touch with the real world while working on these projects. I am very happy to

have met and spent wonderful times with Karen Willey, Anca Miron, Rosa M. Salazar de Peterson, Marina Anciães, Heather York, Elisa Bonaccorso, Juan Manuel Guayasamin, Ismael Hinojosa-Díaz, Alexis Powell, Kris McNyset, Enrique Martínez-Meyer, Elena Brebenel, Yoshi Nakazawa Ueji, Muir Eaton, Michelle Wilkinson, Richard Williams, Ryan Lash, Charles Linkem, Matt Davis, Francine Abe, Jeet Sukumaran, Narayani Barve, and Andrés Lira. I am hopeful that some of the friendships I have made during graduate school will survive time passing and physical distance.

Thanks to the persons who have helped along the way, too many to mention. My sincere gratitude goes to all of you not named here.

TABLE OF CONTENTS

Abstract	iii
Acknowledgements	iv
Chapters:	
1. Vegetation Seasonality and Movement Patterns of a Tropical Frugivorous Bird: Clues from Remotely Sensed Vegetation Indices and Ecological Niche Modeling	1
2. Using Hyperspectral Satellite Imagery for Regional Inventories: a Test with Tropical Emergent Trees from the Amazon Basin	31
3. Seasonal Variation in Species-Specific Spectral Signatures of Rainforest Trees in Southeastern Peru	64

CHAPTER I

Vegetation Seasonality and Movement Patterns of a Tropical Frugivorous Bird: Clues from Remotely Sensed Vegetation Indices and Ecological Niche Modeling

The dynamics of tree phenology represent a major determinant in the structure and function of forest ecosystems. In tropical regions, variation in availability of food resources such as fruit plays an important role in determining temporal, localized changes in animal communities. In Costa Rica, studies in the Caribbean lowlands (Levey 1988), in lower montane forest (Wenny and Levey 1998), and in higher-elevation premontane wet forests (Loiselle and Blake 1991) depicted complex patterns of tree and shrub fruiting. Previous studies have concluded that fruit availability affects seasonal movements and elevational shifts of frugivorous birds, including records in quetzals (*Pharomachus* spp.), bellbirds (*Procnias* spp.), manakins (Pipridae), and euphonias (Blake and Loiselle 2002; Blake et al. 1990; Levey 1988; Loiselle and Blake 1991; Powell and Bjork 1995; Powell and Bjork 2004; Skutch 1969; Slud 1964). Blake and Loiselle (2002) summarized the situation as, “we know relatively little about actual movement patterns and home-range sizes of most frugivores.”

One of the few seasonal migrations that has received much-needed investigation is that of the Three-wattled Bellbird (*Procnias tricarunculata*; Powell

and Bjork 2004), a canopy frugivorous cotinga classified as Vulnerable, ranging from Nicaragua to Panama (BirdLife International 2008). Three distinct song types are recognized for this species (Kroodsma 2005), each in a different breeding area: one song type in northern Nicaragua and southern Honduras (“Nicaraguan” song type); another in the Tilarán Mountains of north-central Costa Rica (“Monteverde”); and a third in the Cordillera de Talamanca of southeastern Costa Rica and western Panama (“Panamanian”). Telemetry studies of a bellbird population breeding in Monteverde Cloud Forest Reserve (above 1300 m) revealed that individuals shift both in elevation and spatially (Powell and Bjork 2004; Fig. 1). Outside of the breeding season, radio-tagged individuals were found on both the Pacific and Atlantic slopes, in both Costa Rica and Nicaragua. The study focused on migration patterns and implications for conservation in this population, including lack of protection of areas used outside of the breeding season; factors determining migration remain unknown, but are presumed to be related to variation in food resource availability and rainfall, which was one important impetus for this study.

The effects of environmental variability on animal movements have been studied via climatic dimensions in ecological niche modeling (ENM) approaches, addressing short and long distance migration in monarch butterflies (Batalden et al. 2007), and austral migration (Joseph and Stockwell 2000) and Nearctic-Neotropical migration (Martínez-Meyer et al. 2004; Nakazawa et al. 2004) in birds. While monarch butterflies wintering ranges showed a shift in the ecological dimensions of breeding ranges, many birds studied tracked the same ecological regimes between

breeding ranges in North America and wintering ranges in Central and South America (“niche followers”); a smaller subset of the species studied changed their ecological conditions between the two seasons (“niche switchers”). Such findings support the hypothesis that long distance, seasonal migration evolved in bird populations locally tracking resources (Levey and Stiles 1992).

The aims of this study are twofold: (1) to investigate the relationship between vegetation seasonality and known movement patterns of the Monteverde bellbird population, and (2) to predict the potential distribution of a different population, for which no information regarding breeding sites or migration patterns is available. Toward the first objective, we analyzed the variation in the Enhanced Vegetation Index (EVI; Huete et al. 1994) derived from the satellite Moderate Resolution Imaging Spectroradiometer (MODIS), as related to known migration sites. Vegetation indices have been shown to correlate well with phenological changes in temperate forests (Fisher and Mustard 2007; Studer et al. 2007; Zhang et al. 2003); in tropical areas, vegetation indices are able to capture phenological differences in the canopies between dry and wet seasons (Huete et al. 2002; Xiao et al. 2006). Hence, here, we compared sites used by Monteverde bellbirds at different times of the year in terms of EVI variability, to assess whether such variation exists, and if it correlates with observed seasonal migration patterns.

Toward the second objective, we focused on a population that resides part of the year in Corcovado National Park, Costa Rica, of the Panamanian song type. Assuming constancy of species ecological characteristics throughout the year

(Nakazawa et al. 2004), we applied ENM to estimate potential distributions for breeding and non-breeding seasons, based on observed occurrences and vegetation indices as input data. Vegetation indices have been used in remote sensing studies to estimate canopy characteristics, such as leaf area index, and chlorophyll and water content (Houborg et al. 2007). In ENM, the Normalized Difference Vegetation Index (NDVI; Tucker 1979) has been used successfully, as vegetation seasonality and type parameter, to address diverse challenges (Cayuela et al. 2006; Ferreira de Siqueira et al. 2009; Osborne et al. 2001; Osborne and Suárez-Seoane 2007; Peterson et al. 2005; Roura-Pascual et al. 2004; Sarasola et al. 2008); more recently, Leaf Area Index (LAI; Chen et al. 1997) has been used to estimate vegetation productivity in studies predicting species' distributions in the Neotropics (Buermann et al. 2008; Prates-Clark et al. 2008).

We include in this study three vegetation indices, two new to the ENM framework. The aim is to describe canopy characteristics and phenological changes between seasons that may influence the movements of bellbirds. Since the migration patterns of this species remain largely unknown, this study provides a first-pass assessment of the potential areas used throughout the year.

1. Methods

1.1. Bellbird seasonal movements and EVI variation

We followed Powell and Bjork (2004) in delineating sites used by Monteverde bellbirds through the year, as follows. Three stages are well defined (Fig. 1, Table 1):

breeding in Monteverde Cloud Forest Reserve (April to June), migration to the Atlantic lowlands of northern Nicaragua (October to December), and migration to the Pacific lowlands in Costa Rica (December to March). We randomly selected 10% of the total number of 500 m resolution pixels inside polygons delineating each distributional area (Fig.1). Similarly, we selected random pixels from across the larger regions of the Pacific and Atlantic lowlands and the middle elevations (1000 - 1800 m), representing ~5% of the total number of pixels.

The two sets of pixels were used to compare MODIS EVI temporal variability between regions and sites visited by bellbirds. EVI is calculated as a ratio between red, blue, and near infrared reflectance channels, and was developed for measuring photosynthetic activity in high biomass regions; the blue channel is used to reduce atmospheric influences (Huete et al. 2002). Since the Monteverde population study was carried out in 1992 - 1995, but MODIS became functional only in 2000 (Justice et al. 2002), we used EVI 16-day time series for year 2004, at 500 m resolution. We choose year 2004 to match the timing of our observations of another population of bellbirds, in Corcovado National Park (see below). None of the two periods (1992-1995 and 2004) was recorded as either moderate or strong El Niño or La Niña years (<http://ggweather.com/enso/oni.htm>), so average rainfall should be comparable. Two 16-day average EVI datasets were available for download for each month of 2004 with two exceptions (January and November), of which only one 16-day average dataset was available. We also used a MODIS land cover product expressed as plant functional type (Sun and Liang 2008), which we downloaded for year 2004 at 500 m

resolution (<https://lpdaac.usgs.gov/>); this dataset was used to mask areas not holding forest. We calculated basic statistics (mean, median, minimum, and maximum) of EVI values to assess temporal variation at the regional and bellbird site scales.

1.2. Ecological niche modeling – algorithms and data input

Ecological niche modeling tools have been applied to investigate various aspects of species distribution and ecology (Araújo et al. 2008; Gaubert et al. 2006; Nyári et al. 2006; Oberhauser and Peterson 2004; Pearson and Dawson 2005; Peterson 2003, 2006a, b; Peterson et al. 2007; Peterson et al. 1999; Raxworthy et al. 2003; Thuiller et al. 2005; Ullah et al. 2007). We use the term “niche” according to Grinnell (1917): the set of environmental conditions that determines a species distribution. Different techniques, from simple bioclimatic envelopes and logistic regressions to more complicated neural networks and genetic algorithms, require sets of known presences and environmental data in the form of raster grids to build models of a species ecological niche. We applied two different ecological niche modeling tools, Genetic Algorithm for Rule Set Projection (GARP, Stockwell and Peters 1999) and maximum entropy (Maxent, Phillips et al. 2006), to study seasonal changes in the ecological distribution of bellbirds observed at Corcovado National Park, Costa Rica.

GARP generates rules about species’ environmental requirements based on presence points and associated environmental data, tests these rules with other known presences, and then modifies and tests again the rules, in an iterative process. The best set of rules (i.e., those that best explain the given data, tested via fitness

functions) is then projected onto geography to estimate the species' potential distribution. We used the DesktopGARP implementation, and ran 100 models with a 50% split of occurrence data into training (model building) and testing (of models produced) sets. Following the recommendations of Anderson et al. (2003) for selecting optimal models, we ran 100 models and used an omission error threshold of 20% of distribution, and commission error of 50 % of distribution. Omission error is calculated based on known presences predicted absent, which can generally be regarded as a model failure. Commission error is based on the areas predicted present for which no known presences are available, thus not necessarily a model failure, and as such a wider range of commission error values is acceptable (Anderson et al. 2003).

We also employed Maxent, a modeling tool based on the Gibbs probability distribution function, to find the maximum entropy distribution: the most spread-out probability distribution given a set of constraints (Phillips et al. 2006). The constraints, called features, are derived from the input environmental variables, and can be linear (unmodified variables), quadratic (variables squared), product (product of two variables), threshold (binary transformation of a variable using a threshold), and hinge (variable constant below a threshold). The optimal combination of features depends on the number of presence points available; the "auto" setting on the Maxent interface allows the program to select the features to be used based on the number of occurrences available. Fewer feature types are used when few presence points are available; model complexity increases when larger presence datasets are available.

We used Maxent 3.1.0, with the default settings for most parameters, including the regularization multiplier, which controls the commission error of the models. The default options have been optimized recently using datasets that varied in complexity and geographic representation (Phillips and Dudík 2008). We used the “raw” output option, which generates models with original probability distribution values (as opposed to logistic or cumulative transforms), and a 50% random split of the presence points into training and testing of predictions.

Occurrence data used in modeling characterized spatial positions of individuals from the population of bellbirds that occupies an area close to the Pacific coast on the Osa Peninsula (Fig. 1), in Corcovado National Park. We observed males calling from subcanopy perches in 14 - 25 March 2004, and recorded their locations using geographic positioning systems (GPS). In all, we accumulated 18 GPS locations of adult and immature males. All adult males sang the Panamanian dialect.

For environmental variables we downloaded MOD13Q1 MODIS data products for 2004, at 250 m resolution. The tiles covering Nicaragua, Costa Rica, and Panama were mosaicked to match the approximate extent of the species' distribution, and reprojected to geographic projection using Modis Reprojection Tool version 4.0 (<https://lpdaac.usgs.gov/lpdaac/>); the same application was used to extract relevant layers (EVI, reflectance bands, and pixel reliability quality assurance). We masked out all pixels flagged as cloud-contaminated in the pixel reliability dataset. MODIS bands from the red (band 1), near infrared (band 2), and middle infrared (band 7) ranges were used to calculate in ENVI 4.5 (ITT Visual Information Solution) the Red

Index (RI, Gitelson et al. 2005) and the Normalized Difference Water Index (NDWI, Gao 1996) as

$$RI = (\text{band 2} / \text{band 1}) - 1$$

$$NDWI = (\text{band 2} - \text{band 7}) / (\text{band 2} + \text{band 7})$$

EVI, RI, and NDWI have been shown to estimate leaf area index, chlorophyll content, and vegetation water content, respectively (Houborg et. al 2007). We considered these canopy parameters to be informative regarding vegetation phenological stages. Based on the timing of the known Monteverde population migration phases, we generated nine environmental datasets for ENM experiments for Corcovado bellbirds, each dataset containing the above three vegetation indices for the time period selected (Table 1). To train models, we used vegetation indices for the first two weeks and last two weeks of March separately, to coincide with our field observations. We used this approach to account for the fact that any vegetation changes occurring between beginning and end of March do not trigger seasonal movements of bellbirds. The extent of these two datasets was set to Osa Peninsula (Fig. 1) as an assumption of the population's mobility, which defined areas for pseudoabsence sampling (Stockwell and Peterson 2002) required in both GARP and Maxent. Selecting a subset of the overall model training region for ENM implies reduced mobility of species and limits the algorithms to exploring a subset of the species' space of potentially suitable abiotic conditions (Soberón and Peterson 2005).

However, our aim was that of modeling the ecological niche of Corcovado population and exploring its spatial and temporal variability. As such, we projected the two March models separately onto the other seven datasets, across an area extending from Nicaragua to Panama. We intersected the two resulting outputs for each period to map areas predicted as suitable in both cases, using the lowest presence threshold approach (Pearson et al. 2007): the model output suitability value at which all known occurrences are predicted present. This approach allowed for changing both Maxent's continuous outputs (probability distribution values) and GARP's categorical ones (model agreement values) to binary outputs (presence-absence) under a 0% omission threshold. All analyses were run separately for GARP and Maxent models in ArcGIS 9.2 (ESRI Inc.).

1.3. GARP and Maxent models – analyzing Corcovado bellbird migration patterns

Our aim was to generate time-dependent potential distributions for birds observed in Corcovado National Park in March 2004, to track seasonal variations in potential areas of occupancy, and to analyze them based on known migration patterns of the Monteverde population. For the latter purpose, we looked at the proportion of area predicted present at the seven different times of the year by region: Osa Peninsula, Pacific lowlands, and Atlantic lowlands, and at elevations of 1000 - 1800 m, the latter to represent the altitudinal component, as described in the migration of Monteverde bellbirds. We calculated numbers of pixels predicted present, out of the total number of pixels available; given that cloud cover varied between time periods, the total

number of pixels available for modeling was not always the same. For this reason, we calculated the number of masked cloud pixels for each time period, and used these numbers to establish lower bounds (i.e., if all cloud pixels were predicted absent) and upper bounds (i.e., if all cloud pixels were predicted present) of proportional areas predicted present.

2. Results

2.1. EVI variation at Monteverde bellbird population sites

We noted different patterns of EVI seasonal variation in the descriptive statistics between regions (Fig. 2). Forests on the Atlantic lowlands were less variable in terms of mean EVI values, which remained around 5000 throughout the year. Clearer separation between seasons was observed in the Pacific lowlands, where average EVI values did not exceed 5000 until late in the season (May), most likely due to the differences in rainfall and consequently pronounced dry and wet seasons. Even more variable are middle elevations: here, mean EVI values remained largely < 5000 from January to July, but then rose between August and October.

Monteverde birds are present in the Atlantic lowlands of southeastern Nicaragua between the end of October and December (Fig. 1), during which time the mean and range of EVI values of areas that they use match those of the overall Atlantic region (Fig. 2). However, sites they use between January and March in the Pacific region are less typical of the broader Pacific lowlands region, being generally higher than surrounding areas (Fig. 2). Their middle elevation breeding site

(Monteverde Cloud Forest reserve) does not match the observed regional mean EVI values: rather, it is generally represented by a narrow interval of the observed variability; only towards the end of the breeding season (i.e., in June) do the two datasets become comparable in terms of means and overall variation.

2.2. Predicting movement patterns of Corcovado bellbirds

The distributions obtained by summing GARP models based on each of the two environmental datasets for March separately (Table 1) predicted all Corcovado occurrences as suitable at lowest presence threshold of 1 model out of 10; each model individually had zero omission error (based on the testing dataset). Since predicting each occurrence point seemed a trivial task, we elevated the threshold to at least half of the 10 models predicting the species present, thus placing more weight on model agreement. GARP projections identified no suitable areas for the last two time periods (July and October), probably because environmental conditions were markedly different and March models could not be extrapolated onto those conditions. Maxent experiments extrapolated from March conditions, on the other hand, were successful in identifying suitable areas, including at the lowest presence threshold, for all projected time periods.

Aside from this discrepancy, GARP and Maxent predictions were comparable in terms of areas predicted present across regions and time periods (Fig. 3). The proportion of the Osa Peninsula predicted present was higher than any other region in all time periods except December. The Pacific lowlands as a whole decreased in

proportional area predicted present from December to March and increased afterwards. The Atlantic lowlands showed similar trends, although the decrease was less pronounced, probably due to the absence of marked dry-wet seasons. Middle elevations had the smallest areas predicted present; an increase was observed for April to June (breeding season), compared to January and March predictions (non-breeding). This trend was clearer in the GARP predictions. ENM projections were noticeably very restricted for the middle elevations, which seem only marginally suitable for the bellbirds through much of the year.

Cloud cover affected predictions most in May, when the uncertainty of the proportion of area predicted present for all regions was larger than the actual areas predicted present. Maxent predictions for July were also greatly affected by clouds. In October, only the prediction for the Osa Peninsula had very large confidence intervals in response to cloud contamination. Cloud cover made pixel-by-pixel comparisons of predicted distributions across time periods impossible: that is, most pixels were cloud-contaminated during one or more time periods. Clearly, cloud cover remains a major obstacle in obtaining complete satellite images in the Tropics, especially ones with high spatial and temporal resolution.

3. Discussion

The natural history of *Procnias tricarunculata* is not well understood, so any inquiries into seasonal movements must remain subject to assumptions. Indeed, here, the data about breeding season are inferential, as practically no nests have been

described (Snow 2004; Stiles and Skutch 1989). According to Snow (1982), considering frequencies of calls and courtship displays, the breeding season probably lasts from February to July. Stiles and Skutch (1989) estimated that the breeding season might last from March to June, based on gonadal measurements from museum specimens and on display records. The limited numbers of specimens and limited locality data are inadequate to permit even a rough estimate of movement patterns, or breeding or seasonal distributions. Indeed, the information available is also often contradictory: e.g., high elevation records on Tenorio and Miravalles volcanoes during the non-breeding season (Slud 1964) and museum specimens from Irazú volcano in February. Given this paucity of information, the present study is intended to provide initial information on spatiotemporal environmental variation, from a bellbird's point of view.

Our analysis of vegetation seasonality expressed through EVI for known seasonal distributional areas of Monteverde bellbirds showed that the Atlantic distributional area correlates with the general, regional variability patterns, whereas the Pacific sites are less representative of the region's phenology. The breeding site in the middle elevation range overlaps with a narrow subset of available seasonal vegetation dynamics. As such, the extent of suitable conditions at this site seems to be very restricted in terms of acceptable variation in the EVI.

Similarly, only a small percentage of the middle elevation areas was predicted as suitable for the Corcovado population of bellbirds when analyzed using ENM tools. It may be possible that breeding areas at middle elevations present a much-

reduced manifestation of the general conditions that are suitable for the bellbirds. According to previous ENM applications to migratory birds (Joseph and Stockwell 2000; Nakazawa et al. 2004), if Corcovado bellbirds track the same suite of ecological conditions through time (“niche followers”), across the Atlantic and Pacific lowlands, these patterns are comparable to Monteverde population movements. That, as in our models identified by ecological requirements, breeding areas show much-reduced potential areas compared with non-breeding season is intriguing, suggesting that (if the species is a niche follower) reasons other than vegetation phenology and food resources may take the birds to the middle elevations to breed. Fretwell (1980) suggested that birds migration behavior evolved to avoid nest predation; nest predation has been suggested as an alternative explanation to seasonality of food resources for altitudinal migration in the Tropics (Loiselle and Blake 1991). A recent study (Boyle 2008) tested this hypothesis on an altitudinal gradient in Costa Rica using artificial nests, and found that nest predation declined with increased elevation. Since our ENMs are based entirely on abiotic factors, such biotic interactions are not included in our models.

However, our aim was to estimate ecological niches that allowed us to explore distributional areas apparently suitable for bellbirds at different times of the year, from the standpoint of vegetation seasonality. Our results show that the Pacific and Atlantic lowlands are more broadly suitable than middle elevations at all times of the year analyzed. Biotic factors such as elevated nest predation in the lowlands may thus provide an explanation for the suitability patterns described via ENM, in contrast with

those observed for the Monteverde population via radio-tracking of individuals. However, we equally cannot eliminate the possibility that Corcovado bellbirds may not favor middle elevations for breeding, in which case our predicted distributions might indeed be correct. Since we have no field data regarding breeding or seasonal movements, we cannot refute the hypothesis of Corcovado bellbirds breeding at elevational ranges different than Monteverde bellbirds. This alternative implies that additional field research is necessary to establish with certitude the breeding sites for this population.

Our findings support the previous concerns regarding the anthropogenic pressure on lowland forests, and the importance of these ecosystems during the non-breeding season for the bellbirds (Powell and Bjork 2004), as well as for many other altitudinal migrants (Loiselle and Blake 1991; Powell and Bjork 1995; Rosselli 1994; Stiles 1983). Given that lowland forests in Costa Rica have experienced the highest deforestation rates in the past two decades (Sánchez-Azofeifa et al. 2001), and in light of the reduced potential distributional areas identified by the ENMs, the future of the bellbirds is likely to be very challenging. The three-wattled bellbird was added to the list of threatened birds of Costa Rica over a decade ago (Collar et al. 1994). Its vulnerable status requires concentrated conservation efforts; however, the large gap of information about the biology and migration of this species will affect the efficiency of conservation measurements undertaken.

REFERENCES:

- Anderson, R.P., Lew, D., & Peterson, A.T. (2003). Evaluating predictive models of species' distributions: Criteria for selecting optimal models. *Ecological Modelling*, 162, 211-232
- Araújo, M.B., Nogués-Bravo, D., Diniz-Filho, J.A.F., Haywood, A.M., Valdes, P.J., & Rahbek, C. (2008). Quaternary climate changes explain diversity among reptiles and amphibians. *Ecography*, 31, 8-15
- Batalden, R.V., Oberhauser, K., & Peterson, A.T. (2007). Ecological niches in sequential generations of eastern North American monarch butterflies (Lepidoptera: Danaidae): the ecology of migration and likely climatic change implications. *Environmental Ecology*, 36, 1365-1373
- BirdLife International (2008). *Species factsheet: Procnias tricarunculatus*: BirdLife International, <http://www.birdlife.org>
- Blake, J.G., & Loiselle, B.A. (2002). Manakins (Pipridae) in second-growth and old-growth forests: Patterns of habitat use, movement, and survival. *Auk*, 119, 132-148
- Blake, J.G., Stiles, F.G., & Loiselle, B.A. (1990). Birds of La Selva Biological Station: Habitat use, trophic composition, and migrants. In A.H. Gentry (Ed.), *Four Neotropical Forests* (pp. 161-182). New Haven: Yale University Press
- Boyle, W.A. (2008). Can variation in risk of nest predation explain altitudinal migration in tropical birds? *Oecologia*, 155, 397-403

- Buermann, W., Saatchi, S.S., Smith, T.B., Zutta, B.R., Chaves, J.A., Milá, B., & Graham, C. (2008). Predicting species distributions across the Amazonian and Andean regions using remote sensing data. *Journal of Biogeography*, *35*, 1160-1176
- Cayuela, L., Benayas, J.M., Justel, A., & Salas-Rey, J. (2006). Modelling tree diversity in a highly fragmented tropical montane landscape. *Global Ecology and Biogeography*, *15*, 602-613
- Chen, J.M., Rich, P.M., Gower, S.T., Norman, J.M., & Plummer, S. (1997). Leaf area index of boreal forests: theory, techniques, and measurements. *Journal of Geophysical Research*, *102*, 29429-29443
- Collar, N.J., Crosby, M.J., & Stattersfield, A.J. (1994). *Birds to watch II: The world list of threatened birds*. Cambridge, UK: BirdLife International
- Ferreira de Siqueira, M., Durigan, G., de Marco Júnior, P., & Peterson, A.T. (2009). Something from nothing: using landscape similarity and ecological niche modeling to find rare plant species. *Journal for Nature Conservation*, *17*, 25-32
- Fisher, J.I., & Mustard, J.F. (2007). Cross-scalar satellite phenology from ground, Landsat, and MODIS data. *Remote Sensing of Environment*, *109*, 261-273
- Fretwell, D.D. (1980). Evolution of migration in relation to factors regulating bird numbers. In K. A. & M. E.S. (Eds.), *Migrant birds in the Neotropics* (pp. 517-527). Washington, D.C.: Smithsonian Institution Press

- Gao, B.C. (1996). NDWI - A normalized difference water index for remote sensing of vegetation liquid water from space. *Remote Sensing of Environment*, 58, 257-266
- Gaubert, P., Papes, M., & Peterson, A.T. (2006). Natural history collections and the conservation of poorly known taxa: Ecological niche modeling in central African rainforest genets (*Genetta* spp.). *Biological Conservation*, 130, 106-117
- Gitelson, A.A., Viña, A., Ciganda, V., Rundquist, D.C., & Arkebauer, T.J. (2005). Remote estimation of canopy chlorophyll content in crops. *Geophysical Research Letters*, 32, L08403
- Grinnell, J. (1917). Field tests of theories concerning distributional control. *American Naturalist*, 51, 115-128
- Houborg, R., Soegaard, H., & Boegh, E. (2007). Combining vegetation index and model inversion methods for the extraction of key vegetation biophysical parameters using Terra and Aqua MODIS reflectance data. *Remote Sensing of Environment*, 106, 39-58
- Huete, A., Didan, K., Miura, T., Rodriguez, E.P., Gao, X., & Ferreira, L.G. (2002). Overview of the radiometric and biophysical performance of the MODIS vegetation indices. *Remote Sensing of Environment*, 83, 195-213
- Huete, A., Justice, C., & Liu, H. (1994). Development of vegetation and soil indexes for MODIS-EOS. *Remote Sensing of Environment*, 49, 224-234

- Joseph, L., & Stockwell, D.R.B. (2000). Temperature-based models of the migration of Swainson's Flycatcher (*Myiarchus swainsoni*) across South America: a new use for museum specimens of migratory birds. *Proceedings of the Academy of Natural Sciences of Philadelphia*, 150, 293-300
- Justice, C.O., Townshend, J.R.G., Vermote, E.F., Masuoka, E., Wolfe, R.E., Saleous, N., Roy, D.P., & Morisette, J.T. (2002). An overview of MODIS Land data processing and product status. *Remote Sensing of Environment*, 83, 3-15
- Kroodsma, D.E. (2005). *The singing life of birds: The art and science of listening to birdsong*. Boston: Houghton Mifflin
- Levey, D. (1988). Spatial and temporal variation in Costa Rican fruit and fruit-eating bird abundance. *Ecological Monographs*, 58, 251-269
- Levey, D.J., & Stiles, F.G. (1992). Evolutionary precursors of long-distance migration: resource availability and movement patterns in Neotropical landbirds. *American Naturalist*, 140, 467-491
- Loiselle, B.A., & Blake, J.G. (1991). Temporal variation in birds and fruits along an elevational gradient in Costa Rica. *Ecology*, 72, 180-193
- Martínez-Meyer, E., Peterson, A.T., & Navarro-Sigüenza, A.G. (2004). Evolution of seasonal ecological niches in the *Passerina* buntings (Aves: Cardinalidae). *Proceedings of the Royal Society B*, 271, 1151-1157
- Nakazawa, Y., Peterson, A.T., Martínez-Meyer, E., & Navarro-Sigüenza, A.G. (2004). Seasonal niches of Nearctic-Neotropical migratory birds: Implications for the evolution of migration. *Auk*, 121, 610-618

- Nyári, A., Ryall, C., & Peterson, A.T. (2006). Global invasive potential of the House Crow (*Corvus splendens*) based on ecological niche modelling. *Journal of Avian Biology*, 37, 306-311
- Oberhauser, K.S., & Peterson, A.T. (2004). Modeling current and future potential wintering distributions of eastern North American monarch butterflies. *Proceedings of the National Academy of Sciences USA*, 100, 14063-14068
- Osborne, P.E., Alonso, J.C., & Bryant, R.G. (2001). Modelling landscape-scale habitat use using GIS and remote sensing: a case study with great bustards. *Journal of Applied Ecology*, 38, 458-471
- Osborne, P.E., & Suárez-Seoane, S. (2007). Identifying core areas in a species' range using temporal suitability analysis: an example using little bustards *Tetrax tetrax* L. in Spain. *Biodiversity and Conservation*, 16, 3505-3518
- Pearson, R.G., & Dawson, T.P. (2005). Long-distance plant dispersal and habitat fragmentation: identifying conservation targets for spatial landscape planning under climate change. *Biological Conservation*, 123, 389-401
- Pearson, R.G., Raxworthy, C., Nakamura, M., & Peterson, A.T. (2007). Predicting species' distributions from small numbers of occurrence records: A test case using cryptic geckos in Madagascar. *Journal of Biogeography*, 34, 102-117
- Peterson, A., Martinez-Campos, C., Nakazawa, Y., & Martinez-Meyer, E. (2005). Time-specific ecological niche modeling predicts spatial dynamics of vector insects and human dengue cases. *Transactions of the Royal Society of Tropical Medicine and Hygiene*, 99, 647-655

- Peterson, A.T. (2003). Predicting the geography of species' invasions via ecological niche modeling. *Quarterly Review of Biology*, 78, 419-433
- Peterson, A.T. (2006a). Ecological niche modeling and spatial patterns of disease transmission. *Emerging Infectious Diseases*, 12, 1822-1826
- Peterson, A.T. (2006b). Uses and requirements of ecological niche models and related distributional models. *Biodiversity Informatics*, 3, 59-72
- Peterson, A.T., Martínez-Meyer, E., Servin, J., & Kiff, L.F. (2007). Ecological niche modelling and strategizing for species reintroductions. *Oryx*
- Peterson, A.T., Soberón, J., & Sánchez-Cordero, V. (1999). Conservatism of ecological niches in evolutionary time. *Science*, 285, 1265-1267
- Phillips, S.J., Anderson, R.P., & Schapire, R.E. (2006). Maximum entropy modeling of species geographic distributions. *Ecological Modelling*, 190, 231-259
- Phillips, S.J., & Dudík, M. (2008). Modeling of species distributions with Maxent: New extensions and a comprehensive evaluation. *Ecography*, 31, 161-175
- Powell, G.V.N., & Bjork, R. (1995). Implications of intratropical migration on reserve design: A case-study using *Pharomachrus mocinno*. *Conservation Biology*, 9, 354-362
- Powell, G.V.N., & Bjork, R.D. (2004). Habitat linkages and the conservation of tropical biodiversity as indicated by seasonal migrations of three-wattled bellbirds. *Conservation Biology*, 18, 500-509

- Prates-Clark, C.D.C., Saatchi, S.S., & Agosti, D. (2008). Predicting geographical distribution models of high-value timber trees in the Amazon Basin using remotely sensed data. *Ecological Modelling*, 211, 309-323
- Raxworthy, C.J., Martínez-Meyer, E., Horning, N., Nussbaum, R.A., Schneider, G.E., Ortega-Huerta, M.A., & Peterson, A.T. (2003). Predicting distributions of known and unknown reptile species in Madagascar. *Nature*, 426, 837-841
- Rosselli, L. (1994). The annual cycle of White-ruffed Manakin, *Corapipo leucorrhoa*, a tropical frugivorous altitudinal migrant, and its food plants. *Bird Conservation International*, 4, 143-160
- Roura-Pascual, N., Suarez, A., Gomez, C., Pons, P., Touyama, Y., Wild, A., & Peterson, A. (2004). Geographical potential of Argentine ants (*Linepithema humile* Mayr) in the face of global climate change. *Proceedings of the Royal Society of London Series B-Biological Sciences*, 271, 2527-2534
- Sánchez-Azofeifa, G.A., Harriss, R.C., & Skole, D.L. (2001). Deforestation in Costa Rica: Quantitative analysis using remote sensing imagery. *Biotropica*, 33, 378-384
- Sarasola, J.H., Bustamante, J., Negro, J.J., & Travaini, A. (2008). Where do Swainson's hawks winter? Satellite images used to identify potential habitat. *Diversity and Distributions*, 14, 742-753
- Skutch, A.F. (1969). Life histories of Central American birds. Cooper Ornithological Society, Berkeley, California

- Slud, P. (1964). The birds of Costa Rica: Distribution and ecology. *Bulletin of the American Museum of Natural History*, 128, 430
- Snow, D.W. (1982). *The Cotingas*. Ithaca, New York: Cornell University Press
- Snow, D.W. (2004). Family Cotingidae (Cotingas). In J. del Hoyo, A. Elliot & D.A. Christie (Eds.), *Handbook of the Birds of the World*. Barcelona, Spain: Lynx Editions
- Soberón, J., & Peterson, A.T. (2005). Interpretation of models of fundamental ecological niches and species' distributional areas. *Biodiversity Informatics*, 2, 1-10
- Stiles, F.G. (1983). Birds. In D.H. Jenzen (Ed.), *Costa Rican Natural History* (pp. 502-530). Chicago, IL.: University of Chicago Press
- Stiles, F.G., & Skutch, A.F. (1989). *A guide to the birds of Costa Rica*. Ithaca, New York: Cornell University Press
- Stockwell, D.R.B., & Peters, D.P. (1999). The GARP modelling system: Problems and solutions to automated spatial prediction. *International Journal of Geographical Information Science*, 13, 143-158
- Stockwell, D.R.B., & Peterson, A.T. (2002). Controlling bias in biodiversity data. In J.M. Scott, P.J. Heglund & M.L. Morrison (Eds.), *Predicting Species Occurrences: Issues of Scale and Accuracy* (pp. 537-546). Washington, D.C.: Island Press

- Studer, S., Stockli, R., Appenzeller, C., & Vidale, P.L. (2007). A comparative study of satellite and ground-based phenology. *International Journal of Biometeorology*, 51, 405-414
- Sun, W., & Liang, S. (2008). Methodologies for mapping plant functional types. In S. Liang (Ed.), *Advances in land remote sensing*. The Netherlands: Springer
- Thuiller, W., Lavorel, S., Araújo, M.B., Sykes, M.T., & Prentice, I.C. (2005). Climate change threats to plant diversity in Europe. *Proceedings of the National Academy of Sciences USA*, 102, 8245-8250
- Tucker, C.J. (1979). Red and photographic infrared linear combinations for monitoring vegetation. *Remote Sensing of Environment*, 8, 127-150
- Ullah, M.I., Amarnath, G., Murthy, M.S.R., & Peterson, A.T. (2007). Mapping the geographic distribution of *Aglaia bourdillonii* Gamble (Meliaceae), an endemic and threatened plant, using ecological niche modeling. *Biodiversity and Conservation*
- Wenny, D.G., & Levey, D.J. (1998). Directed seed dispersal by bellbirds in a tropical cloud forest. *Proceedings of the National Academy of Sciences USA*, 95, 6204-6207
- Xiao, X.M., Hagen, S., Zhang, Q.Y., Keller, M., & Moore, B. (2006). Detecting leaf phenology of seasonally moist tropical forests in South America with multi-temporal MODIS images. *Remote Sensing of Environment*, 103, 465-473

Zhang, X.Y., Friedl, M.A., Schaaf, C.B., Strahler, A.H., Hodges, J.C.F., Gao, F.,
Reed, B.C., & Huete, A. (2003). Monitoring vegetation phenology using
MODIS. *Remote Sensing of Environment*, 84, 471-475

Table 1: Temporal coverage of environmental datasets used in ecological niche modeling experiments and corresponding stages in the annual cycle of Monteverde population of three-wattled bellbirds. Datasets used for training the models are marked with an asterisk.

Dataset	Time period	Location and status
1	3 - 15 December 2003	Atlantic lowlands, in migration
2	1 - 16 January 2004	Pacific lowlands, in migration
3*	5 - 21 March 2004	Pacific lowlands, in migration
4*	21 March - 5 April 2004	Pacific lowlands, in migration
5	6 - 21 April 2004	Monteverde Reserve, breeding
6	8 - 23 May 2004	Monteverde Reserve, breeding
7	9 - 24 June 2004	Monteverde Reserve, breeding
8	11 - 26 July 2004	Atlantic lowlands, in migration
9	15 - 30 October 2004	Atlantic lowlands, in migration

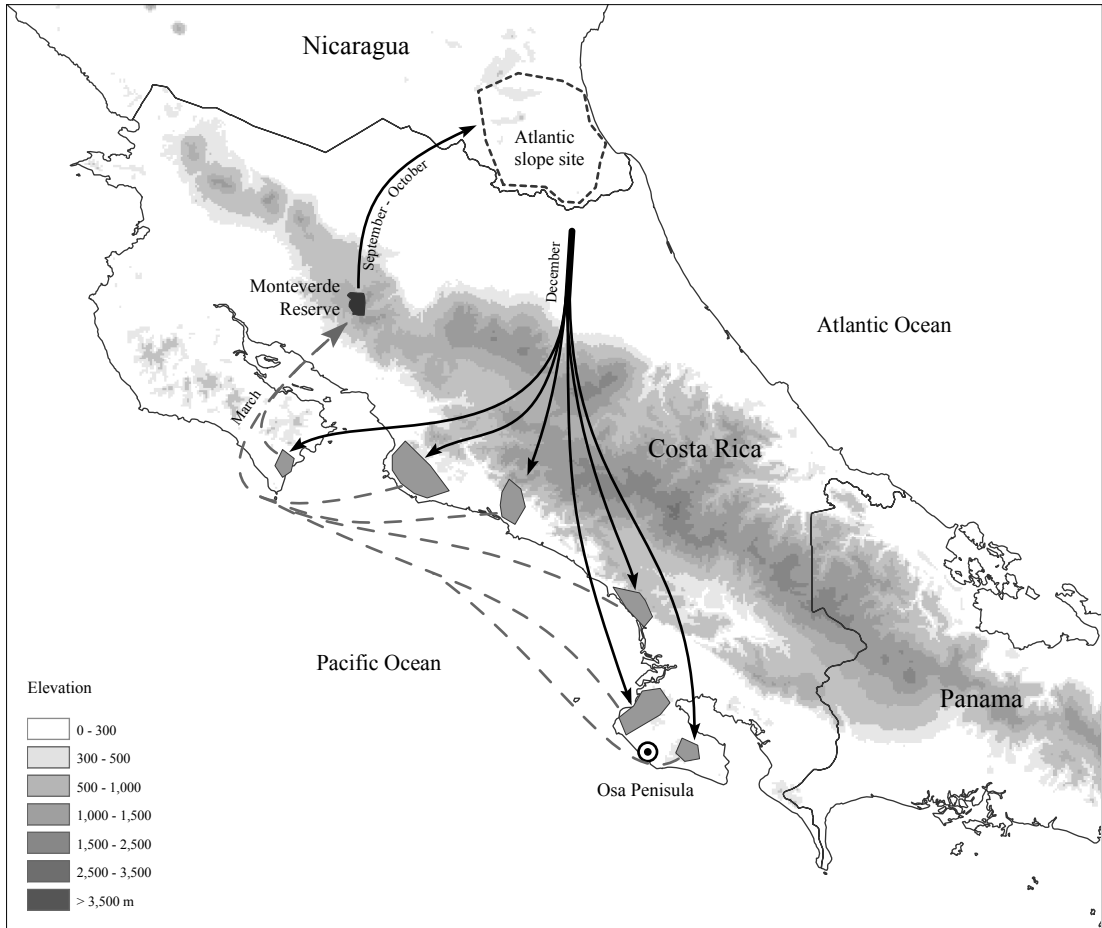


Figure 1: Seasonal migration of Three-Wattled Bellbirds breeding in Monteverde Cloud Forest Reserve, Costa Rica. Pacific lowlands sites are depicted in light gray. Adapted from Powell and Bjork (2004).

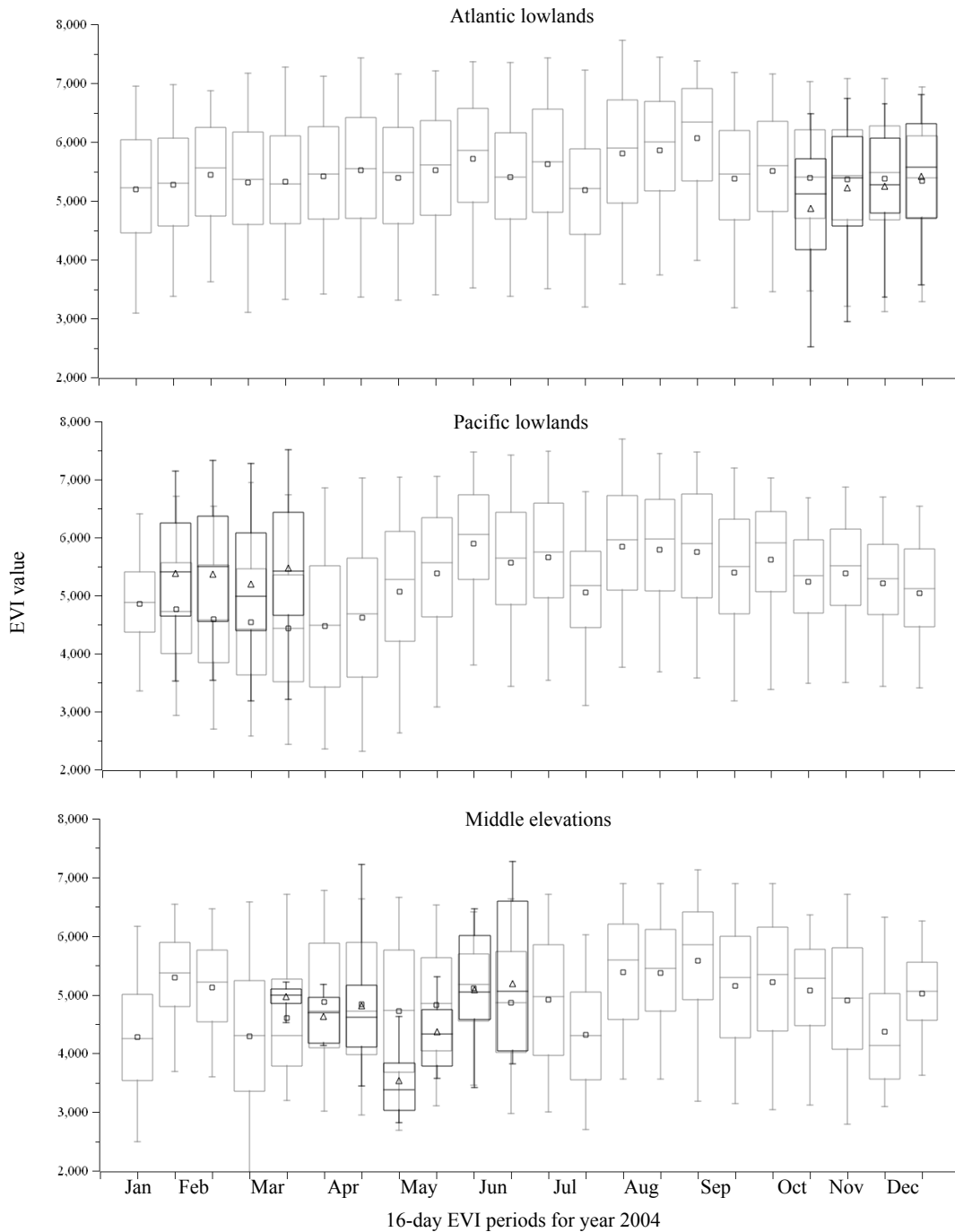


Figure 2: Seasonality of enhanced vegetation index (EVI) across the study region. Regional variation depicted in light gray and specific migration sites in black, with means represented by squares and triangles, respectively; upper quartile corresponds to 75% of values, lower quartile to 25%, and whiskers to 95% and 5%. Two 16-day periods per month were used, except for January and November, each represented by only one 16-day period.

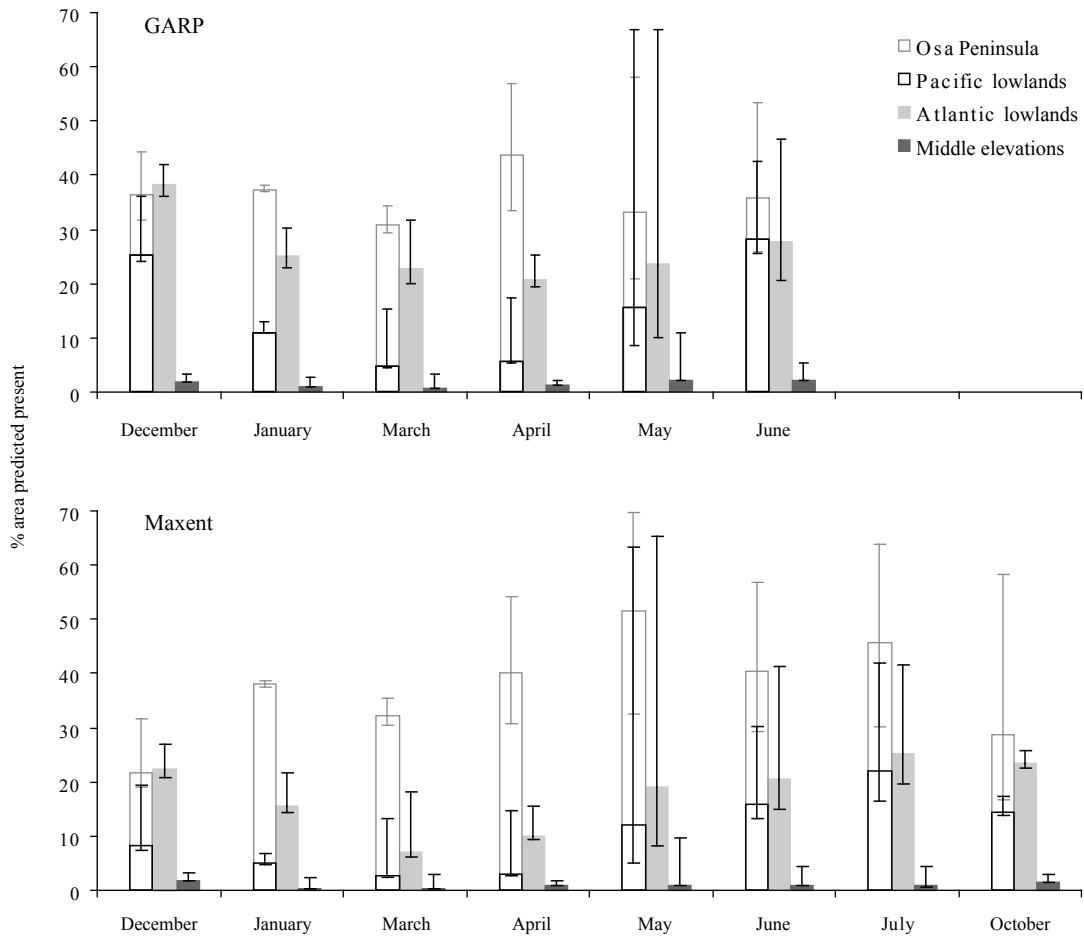


Figure 3: Proportion of regional areas predicted present using ecological niche modeling tools, by region and time period analyzed. Osa Peninsula depicted as a sub-region of the Pacific region. Bars correspond to errors if cloud pixels are considered: upper bar if all cloud pixels predicted present, lower bar if all predicted absent.

CHAPTER II

Using Hyperspectral Satellite Imagery for Regional Inventories: a Test with Tropical Emergent Trees from the Amazon Basin

The field of remote sensing provides powerful tools to address diverse questions in biology. Availability of reliable sources of information-rich satellite imagery like the Landsat platform has enabled study of diverse topics, such as mapping habitat use by caribou (Bechtel et al. 2004), identifying migratory bird habitat (Sader et al. 1991), and comparing tree diversity in protected *versus* logged forests (Foody and Cutler 2003). We are exploring ways in which remote sensing tools can inform the study of tropical frugivorous animals via characterizing availability of resources in time and space (Fleming et al. 1987; Levey 1988; Loiselle and Blake 1991; Price 2004). To understand better the seasonal movements and habitat needs of these animals, much-improved knowledge of the distribution and phenology of tropical trees is necessary. The difficulty, however, lies in the broad, geographic scale of this challenge: detailed phenological studies across significant spatial extents are not feasible. A more desirable approach, if possible, would be to integrate local field studies with remote sensing approaches to scale local-scale results up to the needed landscape-scale perspective.

Here, we attempt to apply this remote sensing approach to understanding tree species distributions in a relatively little-studied but highly diverse area of the Amazon Basin of southeastern Peru thus adding more complexity to the task. However we think that this challenge makes our study more informative for real-life situations. Our goal is to identify canopy trees to species using satellite images collected by a hyperspectral instrument designed to acquire data in hundreds of narrow contiguous spectral bands, procedure termed imaging spectroscopy (Goetz et al. 1985). Hyperspectral data have been used to study different aspects of tropical forest ecosystems for over two decades. Treitz and Howarth (1999) reviewed advances mainly in the study of temperate forest ecosystems after development of airborne sensors such as AVIRIS (Porter and Enmark 1987) and CASI (Anger et al. 1996). The focus then was on detecting or predicting changes of ecosystems through biophysical studies that used band ratio indices and measurements of foliar biochemical content at the leaf and canopy levels. Ecosystem function and structure research based on imaging spectroscopy remains active: recent advances made possible detection, at the forest stand level, of alterations in canopy chemistry owing to invasive species (Asner and Vitousek 2005), mapping species richness using foliar chemistry (Carlson et al. 2007), and classifying mangrove forests (Held et al. 2003). At the leaf level, spectroradiometer measurements quantifying variation in tree foliage in hundreds of bands in the VIS/NIR range (300-1110 nm) have been used to create spectral shapes and separate tropical tree species (Castro-Esau et al. 2006; Cochrane 2000); multiscale studies have combined leaf measurements with airborne

AVIRIS or HYDICE hyperspectral imagery to discriminate temperate (Roberts et al. 2004) or tropical tree species (Clark et al. 2005; Kalacska et al. 2007a; Zhang et al. 2006). Because HYDICE imagery is characterized by high spatial (1.6 m) and spectral resolution (210 bands for the 400-2500 nm region of the spectrum), it was adequate for investigating spectral separation of several tropical tree species at leaf to crown levels. What remains to be established is the extent to which factors like seasonality, flowering and fruiting phenology, canopy epiphyte growth, soil type, and species richness cause intraspecific spectral variation, consequently affecting the capacity of separating tree crowns to species based on spectral signals across landscapes.

Previous research on discriminating tree species used high-resolution airborne imagery; however, obtaining such data for most tropical sites, owing to complicated logistics and high costs, can be impractical. Space platform sensors offer an attractive alternative in terms of costs, temporal resolution, and geographic coverage (Lo and Yeung 2007): at present only one imaging spectrometer, Hyperion, is flown on a space platform, Earth Observing-1 (Ungar et al. 2003). Hyperion gathers data in 224 spectral bands in the 400-2500 nm spectral range, with a spatial resolution of 30 m (Pearlman et al. 2003). As such, this sensor extends the possibility of imaging spectroscopy to any location on Earth. Nevertheless, the sensor has significant shortcomings, such as inevitable cloud cover, relatively coarse spatial resolution, and low signal-to-noise ratios, especially in the shortwave infrared spectrum (Kruse et al. 2002).

Hyperion imagery has been used to study aspects of ecosystem function, such as the importance of precipitation and substrate age (Asner et al. 2005), drought stress (Asner et al. 2004) and phenological variability in tropical forests (Huete et al. 2008), and nitrogen concentration in temperate forest canopies (McNeil et al. 2008; Smith et al. 2003; Townsend et al. 2003). It has also been used to elucidate ecosystem structure, such as estimating tropical forest floristic diversity (Kalacska et al. 2007b), detecting species invasions (Asner et al. 2006; Pengra et al. 2007; Ramsey et al. 2005a; Ramsey et al. 2005b), and characterizing spatial distributions of sugarcane varieties (Galvão et al. 2006) and rainforest types (Thenkabail et al. 2004). To our knowledge, Hyperion has not as yet been used for mapping tree species.

We apply these data resources to the challenge of identifying tropical emergent tree species. This yet to be tested potential use of such data can greatly improve our knowledge of tropical tree diversity and distribution. By using images from dry and wet seasons we take into account seasonal variation of spectra and its implications in discriminating species. Finally, we discuss the advantages and disadvantages of this space-based data source.

1. Materials and Methods

1.1. Study site

The study was carried out in southeastern Peru, Departamento de Madre de Dios, in the watershed of the Río Madre de Dios, along the Río Los Amigos (Fig. 1). The site (70°3'39.96'' W, 12°32'38.40'' S) is part of a larger area under conservation

management by Asociación para la Conservación de la Cuenca Amazónica (ACCA). Three different broad subtypes of tropical lowland evergreen forests can be distinguished in the study area: “aguajal”, dominated by palm trees such as *Mauritia flexuosa* and almost always flooded; “baíjo”, seasonally flooded lowland forests; and “terrazza alta”, which is never inundated (Vega et al. 2006). The climate is humid tropical and rainfall, average 2400 mm annually, is seasonal and lowest in June-September (Osher and Buol 1998).

1.2. Satellite imagery

We used the only satellite-based source of hyperspectral imagery available, Hyperion, an instrument that is part of NASA EO-1 mission. Hyperion imagery has high spectral resolution (channel width of 10 nm, 224 channels) although spatial resolution is only 30 m, which means that trees with small-diameter crowns will be represented by pixels with mixed signals. Given this coarse resolution, locating trees accurately both on the ground and in the imagery is challenging, requiring additional, higher resolution imagery. For this purpose, we opted for panchromatic QuickBird satellite imagery, with spatial resolution of 61 cm, using an image of the study area acquired on 24 June 2006.

Hyperion images of the study area were acquired successfully on 20 July 2006 and again on 29 December 2006 (seven other acquisition attempts in July, October, and December were unsuccessful owing to cloud cover). The images were delivered as Level 1Gst, meaning that they were radiometrically corrected and resampled for

geometric correction and registration to UTM map projection (Simon 2006), and corrections had been applied to remove abnormal pixels and inoperable detectors. However, intermittent pixels with lower values still persist in the images (Goodenough et al. 2003), creating striping in some spectral bands. Another abnormality reported for Hyperion images is the “smile” effect created by an across-track wavelength shift from center wavelength (Goodenough et al. 2003). Although methods to correct for striping and smile effects are available, they are known to alter original spectra (Datt et al. 2003). In addition, because these corrections have to be applied to raw, unprojected images, such preprocessing of images was not practical in our case.

Of the original Hyperion dataset (242 bands), 46 were not calibrated and were removed from the analyses. Examining individual band images and histograms, we further eliminated bands with poor signal-to-noise ratios. As a result, the July and December images were reduced to 130 and 121 spectral bands, respectively (Fig. 2).

We used the FLAASH algorithm (Cooley et al. 2002) available in ENVI 4.2 (RSI, Inc, Boulder, CO, USA) to correct the images atmospherically to transform radiance values to apparent surface reflectance values; this algorithm has been shown to provide results comparable to those of other atmospheric correction packages (Datt et al. 2003). We had to improve the initial registration of the Hyperion images via reference to the QuickBird image. Since no clear landmarks (e.g., road intersections) are available in our study area, we used the outlines of oxbow lakes in an “inverse rubber sheeting” procedure (Dyk et al. 2002): lakes edges visible on the QuickBird

image are moved to fit the pixels representing lakes on the coarser Hyperion imagery. We developed a vector layer of lake boundaries based on the QuickBird image, and used this layer to reduce Hyperion georeferencing error from ≤ 250 m to ≤ 5 m error. This procedure was carried out in Geomatica 10.0 (PCI Geomatics Enterprises, Inc, Richmond Hill, ON, Canada), in the OrthoEngine module.

1.3. Tree samples

Initially, 102 individual trees of 25 genera were selected for study, based on the importance of those tree taxa as food resources for macaws and peccaries (an additional research focus in our group). However, low sample sizes per species reduced the initial list to five taxa of interest, of which only three could easily be identified fully to species: as identifications of the remaining taxa to species was not always possible, they were identified to genus only (Table 1). The GPS position of each tree crown was checked in the field with respect to the QuickBird image. Crowns not identifiable with high confidence on the QuickBird image were removed from the dataset. As such, in the end, we assembled a dataset of five tree genera, each represented by 4-9 individual trees (42 individuals total, see Table 1 and Fig. 1). The small sample sizes are without doubt a constraint on the statistical power of our analyses; however, this situation reflects the challenge of applying experimental tools to real-world circumstances (i.e., little-studied but hyperdiverse forests), where information available can be scarce, as opposed to intensively inventoried sites where individual trees have been tagged and mapped through years of effort.

Another concern related to tree locations was the coincidence of their crowns with the hyperspectral imagery. We checked the (30 m) pixel coverage of each crown (Fig. 3) to assure that crowns were centered in single Hyperion pixels, and identified a subset of crowns that covered $\geq 50\%$ of single Hyperion pixels. We refer to this subset (31 trees) as the “cleaned dataset”, as opposed to the larger “raw dataset” (42 trees; Table 1). Spectra were extracted from Hyperion data (Fig. 4) based on this sampling and were analyzed separately. This approach allowed us to investigate the effects of mixed-signal pixels (i.e., pixels including fragments of different tree crowns) in species identification analyses.

1.4. Statistical analyses

The high dimensionality of hyperspectral imagery and the high likelihood of substantial intercorrelations between channels called for initial reduction of the dimensionality of the imaging spectroscopy datasets (Thenkabail et al. 2004). We employed stepwise discriminant function analysis as a variable selection procedure in SAS 9.1 (SAS Institute Inc., Cary, NC, USA). SAS STEPDISC allows reduction of dimensionality of complex datasets by identifying subsets of variables that contribute most to the discriminatory power of the model, as measured by Wilk’s lambda (Huberty 1994). A particular variable can be removed in one step of the analysis and re-entered in another, since Wilk’s lambda tests for the equality of class means (tree species, in our case) on the selected variable sets iteratively. We used a significance threshold of $\alpha = 0.15$ for variables to enter and be retained in the discriminant function.

The reduced set of spectral channels was then used in a linear discriminant analysis (also performed in SAS 9.1, using the DISCRIM procedure) to test the utility of this information in classifying trees into the correct species and genera. This approach is used commonly in classification studies (Clark et al. 2005; Gong et al. 1997; Rivard et al. 2008; Thenkabail et al. 2004). Clark et al. (2005) showed that linear discriminant analysis reached highest classification accuracy at crown-level resolution when compared with two other classifiers, spectral angle mapper (Kruse et al. 1993) and maximum likelihood (Richards 1999). Discriminant analysis seeks sets of coefficients providing optimal weighted linear composites of scores (discriminant functions, “DFs”) on the predictor variables. The optimal DFs show the highest ratio of between-groups sum of squares to within-groups sum of squares (Warner 2007). In our study, the predictor variables were the narrow bands and the groups (or classes) were the five tree taxa of interest. We ran linear discriminant analyses on both raw and cleaned datasets for both the July and December images. The DISCRIM procedure in SAS provides four multivariate statistic tests of the degree to which the model predicts group memberships better than random: Wilk’s lambda, Pillai’s trace, Hotelling-Lawley trace, and Roy’s greatest root. Classification results were tested using cross-validation, in which each tree crown was omitted sequentially while performing the linear discriminant analyses, and the ability of the model to predict the crown left out is taken as a measure of the predictive power of the model. We also used the CANDISC procedure to derive canonical variables representing linear combinations of the original variables (spectral bands) that best summarize

differences among species. The first two canonical variables were used to graph positions of individual trees and class means to understand discrepancies between posterior probability values and cross-validation tests.

Finally, to test whether landscape-level predictions derived from the two seasonal datasets are consistent between seasons, we applied the DFs to a broader swath of the Hyperion dataset for each season, and analyzed correspondence between seasons in terms of pixels classified as each taxon via a binomial test. DFs were developed using the cleaned datasets with five classes (the five taxa), plus a non-target class that included individuals of four other genera of emergent trees and patches of bamboo and palms that we had mapped. This analysis was carried out on an area centered on our study site, covering ~12 km of the total available image length of 105 km (Fig. 4). We calculated (a) the number of pixels classified as the same taxon in the two datasets, July and December (n_i , where i = five taxa), and (b) the number of pixels for which one or more of the eight adjacent pixels was classified as the same taxon (n_{8i}). (We included the latter index focused on neighboring pixels in the analysis to account for possible errors in registration between the two seasons.)

Numbers of pixels selected under the two criteria were used to calculate a binomial probability p of the observed degree of coincidence being achieved at random. Specifically, we calculated the probability of encountering at least one correct match (out of 9 possibilities) between the two seasonal datasets for each species at random given simple frequencies of occurrence of pixels classified as a taxon as

$$p_{iJ9} = 1 - [1 - (n_{iJ} * n_{iD}) / N^2]^9,$$

where p_{iJ9} is the probability of a July pixel (classified as one of the five taxa) being correctly classified in the December dataset when neighborhood pixels are taken into consideration, n_{iJ} is the number of pixels classified as one of the five taxa in the July dataset, n_{iD} is the number of pixels classified as the same taxon in December dataset, and N is the total number of pixels in the analysis. A simpler way to write the formula above is

$$p_{iJ9} = 1 - [1 - (p_{iJ} * p_{iD})]^9,$$

where p_{iJ} is the probability of a pixel being correctly classified as one taxon in July dataset and p_{iD} is the probability of a pixel being correctly classified as the same taxon in December dataset. The binomial test of significance was performed using a binomial distribution with total number of trials n_{iJ} , number of successes $n_i + n_{8i}$, and underlying probability of a success of p_{iJ9} .

2. Results

The stepwise discriminant selection procedure retained 30 narrow bands from the initial set of 130 and 121 for July and December, respectively. The subsets selected from the two images differed in terms of spectral coverage (Fig. 2): most

July channels belonged to the near- and middle-infrared portion of the spectrum, while only half of the December channels belonged to this portion. This result suggests the possibility of phenological differences between the seasons (dry – July, wet – December) expressed in the information content of the images.

Because of the combination of low tree sample sizes and numerous predictor variables, however, we could not incorporate all 30 channels in our analyses. Rather, we used subsets of 25, 15, and 5 channels, in the order that they were selected through the stepwise procedure. Because within-class covariance matrices were singular (i.e., they had a determinant of 0), further discriminant analyses were developed based on pooled covariance matrices.

The linear discriminant analyses yielded markedly different results for raw and cleaned datasets (Table 1). The four multivariate statistics (Wilk's lambda, Pillai's trace, Hotelling-Lawley trace, and Roy's greatest root) testing group membership predictions were all highly significant ($P < 0.0001$) for July and December cleaned datasets represented by 5, 15, and 25 narrow bands, but decreased in significance (in some cases to $P \approx 0.1$) when raw datasets were used. Classification accuracy based on cross-validation tests was very low (<15 % for 25 channels) for raw datasets; however, for cleaned datasets, accuracy was 100% for the five taxa in both seasons when 25 channels were used. Accuracy decreased when fewer channels were used (Table 1).

Nevertheless, inspection of posterior probabilities in the raw dataset showed that only two of the 42 trees had relatively low values ($\leq 90\%$), suggesting that most

of the trees would have been classified correctly. We suspect that some pixels in the raw dataset had mixed spectra corresponding to crowns of individuals of multiple tree species, such that some of these pixels could be closer spectrally to other class centroids than to their “own” class centroids. This scenario would explain the low classification success obtained with cross-validation but high posterior probabilities in the raw dataset analysis.

To explore this assumption further, we plotted the raw and cleaned datasets using the first and second canonical axes derived from the 25 narrow bands used in the linear discriminant analysis (Fig. 5). For the cleaned dataset, the separation of taxa is remarkable—indeed, it appears absolute. In the raw dataset, however, some individual trees fall closer to individuals of other genera than to their own class centroids. For July dataset, these individuals belong to the taxa for which the classification in the raw dataset had the lowest values: *Parkia* sp., *Apuleia leiocarpa*, and *Hymenaea* sp. The information extracted and analyzed from the December dataset produced mostly cohesive groups in the canonical variable space (*Hymenaea* sp. and *Cedrelinga cateniformis*) when the raw dataset was used. Nonetheless, all taxa grouped into nonoverlapping or minimally overlapping clusters corresponding to the correct sets of individuals, even in the raw dataset analyses.

When applying DFs to the broader landscape captured in the Hyperion datasets, over half of the pixels were classified as “other” (i.e., left unclassified), whereas the target taxa were represented by small percentages of the overall area. For the July dataset, ~76% of pixels were unclassified, 2% were identified as the non-

target class, 7% as *Apuleia leiocarpa*, 4% as *Bertholletia excelsa*, 5% as *Cedrelinga cateniformis*, 2% as *Hymenaea* sp., and 4% as *Parkia* sp.; comparably, for the December dataset, ~61% were unclassified, 19% as non-target class, 7% as *Apuleia leiocarpa*, 2% as *Bertholletia excelsa*, 2% as *Cedrelinga cateniformis*, 6% as *Hymenaea* sp., and 3% as *Parkia* sp. Numbers of pixels classified into one or another class varied with the posterior probability threshold applied—in the end, we chose a threshold of 99% based on the initial posterior probabilities of the training data (31 trees). The binomial probabilities associated with observed levels of correspondence between the two datasets in terms of pixels classified as particular species were quite low ($P < 10^{-12}$) for all five species, indicating that the observed degree of matching was highly nonrandom. As such, our landscape-level predictions of taxon distributions that were developed independently from the two seasonal images show consistency in expected distribution patterns.

3. Discussion

Although spectral discrimination of tropical tree species remains an emerging field, advances over the last two decades in understanding leaf optical properties and developing better instruments for imaging spectroscopy have been applied most frequently in mapping trees in areas less diverse and challenging than tropical rain forests (Dennison and Roberts 2003; Gong et al. 1997; Roberts et al. 2004; Townsend and Foster 2002; Underwood et al. 2007). In tropical ecosystems, studies have mapped trees in Costa Rica (Clark et al. 2005; Zhang et al. 2006), mangrove tree

species in Australia (Held et al. 2003), and native and invasive tree species in Hawaii (Asner et al. 2008; Asner et al. 2006).

Mapping trees in tropical systems can be particularly challenging because of high species diversity and lack of imaging spectroscopy. That two pioneering studies focusing on discriminating tropical tree species (Clark et al. 2005; Zhang et al. 2006) used the same imaging spectroscopy datasets underlines the complications of obtaining airborne imaging spectroscopy across much of the Tropics (Castro-Esau and Kalacska 2008). To our knowledge, this study represents the first attempt to use space-borne imaging spectroscopy to discriminate tree species in a diverse tropical rainforest, although Hyperion data have been used in the less diverse forests of Hawaii to differentiate between native and invasive canopy trees based on their biophysical characteristics (Asner et al. 2006).

Compared to the work of Clark et al. (2005) and Zhang et al. (2006), this study is novel in that it shows the potential for analyses of satellite imaging spectroscopy to detect tree species in highly diverse forests. It suggests that opportunities to apply these techniques to lesser studied, more diverse regions of the Tropics exist. However, the only source available for such data, Hyperion, has several significant limitations. As has been noted in several publications (Datt et al. 2003; Goodenough et al. 2003; Kruse et al. 2002), issues such as the relatively coarse resolution, low signal-to-noise ratio, striping, and smile effects, present particular challenges. We also experienced delays in acquisition scheduling and problems with cloud cover. In the course of one year, we scheduled 6 data acquisitions, each

including three attempts to obtain data with <20% cloud cover, but only two of the datasets acquired were usable and scheduling was not always precise. Nevertheless, given the high costs of airborne imaging spectroscopy, satellite imagery probably remains the most accessible solution for collecting hyperspectral data in much of the Tropics.

We focused on solutions to the problem of relatively coarse spatial resolution. Previous studies (Ramsey et al. 2005a; Ramsey et al. 2005b) used subpixel extraction methods to map an invasive tree species that has crowns too small to be represented well by single pixels. Those studies were successful because the species in question generally occupies monospecific patches, but also thanks to the quite-different chemistry and phenology of its foliage compared to native species.

Still, we consider it remarkable that Ramsey et al. (2005b) found only minor differences between field spectra and Hyperion spectra, an avenue that we wish to pursue in future studies. Foliar reflectance is determined by factors such as leaf thickness, pigmentation, and internal structure; at the crown level, lianas and other associated plants can influence light reflected off canopies (Castro-Esau et al. 2004; Castro-Esau et al. 2006; Sánchez-Azofeifa and Castro-Esau 2006). Although we have no field spectra with which to compare our image-derived spectra, our results illustrate that the coarse resolution of Hyperion is sufficient to separate crowns of five genera of emergent trees spectrally. Our results indicate that even mixed-pixel spectra have some ability to separate species, but that mixing does reduce the signal, although we cannot quantify how much of this reduction is an artifact of small and unbalanced

tree samples. Plotting spectra using canonical axes suggests that the classifications based on cross-validation may be weak compared to simple posterior-probability classification, owing to a few mixed pixels in the raw dataset that can bias the cross-validation analysis.

We attempted landscape-level classification of Hyperion datasets using the DFs developed based on the cleaned dataset and 25 narrow bands to obtain maps of the species studied. The results are difficult to evaluate given our small samples and the hyperdiverse tree community at the site. The significant overlap in position of pixels classified as particular taxa between the two seasons provides more support for the utility of Hyperion data for mapping tree species. We also observed in the results of these whole dataset classification experiments some regions that presented ordered, linear patterns, most likely artifacts related to striping in some spectral channels (Datt et al. 2003). As such, this application requires further fine tuning and testing, which we hope to achieve via on-ground field surveys of predicted sites for species.

Finally, our study identified different suites of narrow bands as most informative for separation of species and genera between the two seasons. This finding resonates with other recent studies (Asner et al. 2006; Castro-Esau et al. 2006; Dennison and Roberts 2003; Huete et al. 2008) that have emphasized the importance of taking into account seasonality and spectral variability in such analyses. We hope to be able to take advantage of such variability in future work regarding the phenology of these and other target tree taxa.

In sum, we demonstrate that satellite-derived hyperspectral imagery can be used successfully to classify emergent tree species. Three limitations were particularly predominant: (1) acquisition of cloud-free hyperspectral imagery, (2) spatial resolution of the hyperspectral imagery, and (3) sample sizes of identified and georeferenced individual trees—the first two limitations are a function of the sensor and its ability to capture imagery, whereas the third limitation reflects the difficulties of on-ground field work in such remote areas. Our results focus on five genera from among the much greater tree diversity present on the study area. More intensive botanical sampling across the study area could boost sample sizes and make future analyses more robust. Next steps will focus on phenological differences between images captured in different seasons, particularly in light of additional Hyperion data as they become available, and relating results to movements of animal species that use these trees as food resources.

REFERENCES:

- Anger, C.D., Achal, S., Ivanco, T., Mah, S., Price, R., & Busler, J. (1996). Extended operational capabilities of casi. *Proceedings of the 2nd International Airborne Remote Sensing Conference, San Francisco, California.* (pp. 124-133)
- Asner, G.P., Carlson, K.M., & Martin, R.E. (2005). Substrate age and precipitation effects on Hawaiian forest canopies from spaceborne imaging spectroscopy. *Remote Sensing of Environment, 98*, 457-467
- Asner, G.P., Jones, M.O., Martin, R.E., Knapp, D.E., & Hughes, R.F. (2008). Remote sensing of native and invasive species in Hawaiian forests. *Remote Sensing of Environment, 112*, 1912-1926
- Asner, G.P., Martin, R.E., Carlson, K.M., Rascher, U., & Vitousek, P.M. (2006). Vegetation-climate interactions among native and invasive species in Hawaiian rainforest. *Ecosystems, 9*, 1106-1117
- Asner, G.P., Nepstad, D., Cardinot, G., & Ray, D. (2004). Drought stress and carbon uptake in an Amazon forest measured with spaceborne imaging spectroscopy. *Proceedings of the National Academy of Sciences USA, 101*, 6039-6044
- Asner, G.P., & Vitousek, P.M. (2005). Remote analysis of biological invasion and biogeochemical change. *Proceedings of the National Academy of Sciences USA, 102*, 4383-4386
- Bechtel, A., Sánchez-Azofeifa, A., Rivard, B., Hamilton, G., Martin, J., & Dzus, E. (2004). Associations between Woodland Caribou telemetry data and Landsat

TM spectral reflectance. *International Journal of Remote Sensing*, 25, 4813-4827

Carlson, K.M., Asner, G.P., Hughes, R.F., Ostertag, R., & Martin, R.E. (2007).

Hyperspectral remote sensing of canopy biodiversity in Hawaiian lowland rainforests. *Ecosystems*, 10, 536-549

Castro-Esau, C., & Kalacska, M. (2008). Tropical dry forest phenology and

discrimination of tropical tree species using hyperspectral data. In M.

Kalacska & G.A. Sánchez-Azofeifa (Eds.), *Hyperspectral remote sensing of tropical and subtropical forests*. Boca Raton, FL: CRC Press

Castro-Esau, K.L., Sánchez-Azofeifa, G.A., & Caelli, T. (2004). Discrimination of

lianas and trees with leaf-level hyperspectral data. *Remote Sensing of Environment*, 90, 353-372

Castro-Esau, K.L., Sánchez-Azofeifa, G.A., Rivard, B., Wright, S.J., & Quesada, M.

(2006). Variability in leaf optical properties of Mesoamerican trees and the potential for species classification. *American Journal of Botany*, 93, 517-530

Clark, M.L., Roberts, D.A., & Clark, D.B. (2005). Hyperspectral discrimination of

tropical rain forest tree species at leaf to crown scales. *Remote Sensing of Environment*, 96, 375-398

Cochrane, M.A. (2000). Using vegetation reflectance variability for species level

classification of hyperspectral data. *International Journal of Remote Sensing*, 21, 2075-2087

- Cooley, T., Anderson, G.P., Felde, G.W., Hoke, M.L., Ratkowski, A.J., Chetwynd, J.H., Gardner, J.A., Adler-Golden, S.M., Matthew, M.W., Berk, A., Bernstein, L.S., Acharya, P.K., Miller, D., & Lewis, P. (2002). FLAASH, a MODTRAN4-based atmospheric correction algorithm, its application and validation. *Proceedings of the IEEE International Geoscience and Remote Sensing Symposium (IGARSS '02) Toronto (Ontario), Canada, Vol. 3.* (pp. 1414-1418).
- Datt, B., McVicar, T.R., Van Niel, T.G., Jupp, D.L.B., & Pearlman, J.S. (2003). Preprocessing EO-1 Hyperion hyperspectral data to support the application of agricultural indexes. *IEEE Transactions on Geoscience and Remote Sensing, 41*, 1246-1259
- Dennison, P.E., & Roberts, D.A. (2003). The effects of vegetation phenology on endmember selection and species mapping in southern California chaparral. *Remote Sensing of Environment, 87*, 295-309
- Dyk, A., Goodenough, D.G., Bhogal, A.S., Pearlman, J., & Love, J. (2002). Geometric correction and validation of Hyperion and ALI data for EVEOSD. *Proceedings of the IEEE International Geoscience and Remote Sensing Symposium (IGARSS '02), Toronto (Ontario), Canada, Vol. 1.* (pp. 579-583).
- Fleming, T.H., Breiwich, R., & Whitesides, G.H. (1987). Patterns of tropical vertebrate frugivore diversity. *Annual Review of Ecology and Systematics, 18*, 91-109

- Foody, G.M., & Cutler, M.E.J. (2003). Tree biodiversity in protected and logged Bornean tropical rain forests and its measurement by satellite remote sensing. *Journal of Biogeography*, 30, 1053-1066
- Galvão, L.S., Formaggio, A.R., & Tisot, D.A. (2006). The influence of spectral resolution on discriminating Brazilian sugarcane varieties. *International Journal of Remote Sensing*, 27, 769-777
- Goetz, A.F.H., Vane, G., Solomon, J.E., & Rock, B.N. (1985). Imaging spectrometry for Earth remote sensing. *Science*, 228, 1147-1153
- Gong, P., Pu, R.L., & Yu, B. (1997). Conifer species recognition: An exploratory analysis of in situ hyperspectral data. *Remote Sensing of Environment*, 62, 189-200
- Goodenough, D.G., Dyk, A., Niemann, K.O., Pearlman, J.S., Hao, C., Han, T., Murdoch, M., & West, C. (2003). Processing Hyperion and ALI for forest classification. *IEEE Transactions on Geoscience and Remote Sensing*, 41, 1321-1331
- Held, A., Ticehurst, C., Lymburner, L., & Williams, N. (2003). High resolution mapping of tropical mangrove ecosystems using hyperspectral and radar remote sensing. *International Journal of Remote Sensing*, 24, 2739-2759
- Huberty, C. (1994). *Applied discriminant analysis*. New York, NY: Wiley-Interscience
- Huete, A., Kim, Y., Ratana, P., Didan, K., Shimabukoro, Y.E., & Miura, T. (2008). Assessment of phenologic variability in Amazon tropical rainforests using

- hyperspectral Hyperion and MODIS satellite data. In M. Kalacska & G.A. Sánchez-Azofeifa (Eds.), *Hyperspectral remote sensing of tropical and subtropical forests* (pp. 233-259). Boca Raton, FL: CRC Press
- Kalacska, M., Bohman, S., Sánchez-Azofeifa, G.A., Castro-Esau, K., & Caelli, T. (2007a). Hyperspectral discrimination of tropical dry forest lianas and trees: comparative data reduction approaches at the leaf and canopy levels. *Remote Sensing of Environment*, *109*, 406-415
- Kalacska, M., Sánchez-Azofeifa, G.A., Rivard, B., Caelli, T., White, H.P., & Calvo-Alvarado, J.C. (2007b). Ecological fingerprinting of ecosystem succession: estimating secondary tropical dry forest structure and diversity using imaging spectroscopy. *Remote Sensing of Environment*, *108*, 82-96
- Kruse, F.A., Boardman, J.W., Huntington, J.F., Mason, P., & Quigley, M.A. (2002). Evaluation and validation of EO-1 Hyperion for geologic mapping. *Proceedings of the IEEE International Geoscience and Remote Sensing Symposium (IGARSS '02) Toronto (Ontario), Canada, Vol. 1.* (pp. 593-595).
- Kruse, F.A., Lefkoff, A.B., Boardman, J.W., Heidebrecht, K.B., Shapiro, A.T., Barloon, P.J., & Goetz, A.F.H. (1993). The Spectral Image-Processing System (SIPS) - Interactive visualization and analysis of imaging spectrometer data. *Remote Sensing of Environment*, *44*, 145-163
- Levey, D. (1988). Spatial and temporal variation in Costa Rican fruit and fruit-eating bird abundance. *Ecological Monographs*, *58*, 251-269

- Lo, C.P., & Yeung, A.K.W. (2007). *Concepts and techniques of geographic information systems*. Upper Saddle River, NJ: Pearson Prentice Hall
- Loiselle, B.A., & Blake, J.G. (1991). Temporal variation in birds and fruits along an elevational gradient in Costa Rica. *Ecology*, *72*, 180-193
- McNeil, B.E., Read, J.M., Sullivan, T.J., McDonnell, T.C., Fernandez, I.J., & Driscoll, C.T. (2008). The spatial pattern of nitrogen cycling in the Adirondack Park, New York. *Ecological Applications*, *18*, 438-452
- Osher, L.J., & Buol, S.W. (1998). Relationship of soil properties to parent material and landscape position in eastern Madre de Dios, Peru. *Geoderma*, *83*, 143-166
- Pearlman, J.S., Barry, P.S., Segal, C.C., Shepanski, J., Beiso, D., & Carman, S.L. (2003). Hyperion, a space-based imaging spectrometer. *IEEE Transactions on Geoscience and Remote Sensing*, *41*, 1160-1173
- Pengra, B.W., Johnston, C.A., & Loveland, T.R. (2007). Mapping an invasive plant, *Phragmites australis*, in coastal wetlands using the EO-1 Hyperion hyperspectral sensor. *Remote Sensing of Environment*, *108*, 74-81
- Porter, W.M., & Enmark, H.T. (1987). A system overview of the Airborne/Visible/Infrared Imaging Spectrometer (AVIRIS). *Proceedings of SPIE*, *834*, 22-29
- Price, O.F. (2004). Indirect evidence that frugivorous birds track fluctuating fruit resources among rainforest patches in the Northern Territory, Australia. *Austral Ecology*, *29*, 137-144

- Ramsey, E., Rangoonwala, A., Nelson, G., & Ehrlich, R. (2005a). Mapping the invasive species, Chinese tallow, with EO1 satellite Hyperion hyperspectral image data and relating tallow occurrences to a classified Landsat Thematic Mapper land cover map. *International Journal of Remote Sensing*, 26, 1637-1657
- Ramsey, E., Rangoonwala, A., Nelson, G., Ehrlich, R., & Martella, K. (2005b). Generation and validation of characteristic spectra from EO1 Hyperion image data for detecting the occurrence of the invasive species, Chinese tallow. *International Journal of Remote Sensing*, 26, 1611-1636
- Richards, J.A. (1999). *Remote sensing digital image analysis*. Berlin: Springer-Verlag
- Rivard, B., Sánchez-Azofeifa, G.A., Foley, S., & Calvo-Alvarado, J.C. (2008). Species classification of tropical tree leaf reflectance and dependence on selection of spectral bands. In M. Kalacska & G.A. Sánchez-Azofeifa (Eds.), *Hyperspectral remote sensing of tropical and subtropical forests* (pp. 141-159). Boca Raton, FL: CRC Press
- Roberts, D.A., Ustin, S.L., Ogunjemiyo, S., Greenberg, J., Dobrowski, S.Z., Chen, J.Q., & Hinckley, T.M. (2004). Spectral and structural measures of northwest forest vegetation at leaf to landscape scales. *Ecosystems*, 7, 545-562
- Sader, A.S., Powell, G.V.N., & Rappole, J.H. (1991). Migratory bird habitat monitoring through remote sensing. *International Journal of Remote Sensing*, 12, 363-372

- Sánchez-Azofeifa, G.A., & Castro-Esau, K. (2006). Canopy observations on the hyperspectral properties of a community of tropical dry forest lianas and their host trees. *International Journal of Remote Sensing*, 27, 2101-2109
- Simon, K. (2006). Hyperion Level 1Gst (L1Gst) product output files data format control book (DFCB). USGS Center for Earth Resource Observation and Science (EROS), Sioux Falls, S.D.
- Smith, M.L., Martin, M.E., Plourde, L., & Ollinger, S.V. (2003). Analysis of hyperspectral data for estimation of temperate forest canopy nitrogen concentration: comparison between an airborne (AVIRIS) and a spaceborne (Hyperion) sensor. *IEEE Transactions on Geoscience and Remote Sensing*, 41, 1332-1337
- Thenkabail, P.S., Enclona, E.A., Ashton, M.S., Legg, C., & De Dieu, M.J. (2004). Hyperion, IKONOS, ALI, and ETM plus sensors in the study of African rainforests. *Remote Sensing of Environment*, 90, 23-43
- Townsend, P.A., & Foster, J.R. (2002). Comparison of EO-1 Hyperion to AVIRIS for mapping forest composition in the Appalachian Mountains, USA. *Proceedings of the IEEE International Geoscience and Remote Sensing Symposium (IGARSS '02) Toronto (Ontario), Canada, Vol. 2.* (pp. 793-795).
- Townsend, P.A., Foster, J.R., Chastain, R.A., Jr., & Currie, W.S. (2003). Application of imaging spectroscopy to mapping canopy nitrogen in the forests of the central Appalachian Mountains using Hyperion and AVIRIS. *IEEE Transactions on Geoscience and Remote Sensing*, 41, 1347-1354

- Treitz, P.M., & Howarth, P.J. (1999). Hyperspectral remote sensing for estimating biophysical parameters of forest ecosystems. *Progress in Physical Geography*, 23, 359-390
- Underwood, E., Ustin, S., & Ramirez, C. (2007). A Comparison of Spatial and Spectral Image Resolution for Mapping Invasive Plants in Coastal California. *Environmental Management*, 39, 63-83
- Ungar, S.G., Pearlman, J.S., Mendenhall, J.A., & Reuter, D. (2003). Overview of the Earth Observing One (EO-1) mission. *IEEE Transactions on Geoscience and Remote Sensing*, 41, 1149-1159
- Vega, M.S., Ceroni, A., & Reynel, C. (2006). Observaciones ecológicas y taxonomía del género *Codonanthe* (Mart.) Hanst. (Gesneriaceae) en la cuenca del río Los Amigos, Madre de Dios, Perú. *Ecología Aplicada*, 5, 37-43
- Warner, R.M. (2007). *Applied statistics: From bivariate through multivariate techniques*. Thousand Oaks, CA: Sage Publications
- Zhang, J., Rivard, B., Sánchez-Azofeifa, A., & Castro-Esau, C. (2006). Intra- and inter-class spectral variability of tropical tree species at La Selva, Costa Rica: Implications for species identification using HYDICE imagery. *Remote Sensing of Environment*, 105, 129-141

Table 1: Taxa used in this study, with number of individuals and classification success values (percentage) for both raw and cleaned datasets (see Methods), broken down by the three sets of analyses based on different numbers of narrow bands.

Number		Raw dataset			Clean dataset		
of bands	Tree species	N	July	December	N	July	December
5 bands	<i>Apuleia leiocarpa</i>	8	50	12.5	4	75	75
	<i>Bertholletia excelsa</i>	11	27.27	63.64	9	33.33	66.66
	<i>Cedrelinga</i>	10	60	50	8	50	50
	<i>cateniformis</i>						
	<i>Hymenaea</i> sp.	6	0	0	5	40	60
	<i>Parkia</i> sp.	7	28.57	14.29	5	40	20
15 bands	<i>Apuleia leiocarpa</i>	8	12.5	62.5	4	100	100
	<i>Bertholletia excelsa</i>	11	45.45	45.45	9	100	88
	<i>Cedrelinga</i>	10	30	50	8	100	100
	<i>cateniformis</i>						
	<i>Hymenaea</i> sp.	6	16.67	50	5	100	100
	<i>Parkia</i> sp.	7	0	28.57	5	100	60
25 bands	<i>Apuleia leiocarpa</i>	8	25	22.5	4	100	100
	<i>Bertholletia excelsa</i>	11	45.45	18.18	9	100	100
	<i>Cedrelinga</i>	10	50	50	8	100	100
	<i>cateniformis</i>						
	<i>Hymenaea</i> sp.	6	33.33	16.67	5	100	100
	<i>Parkia</i> sp.	7	14.29	14.29	5	100	100

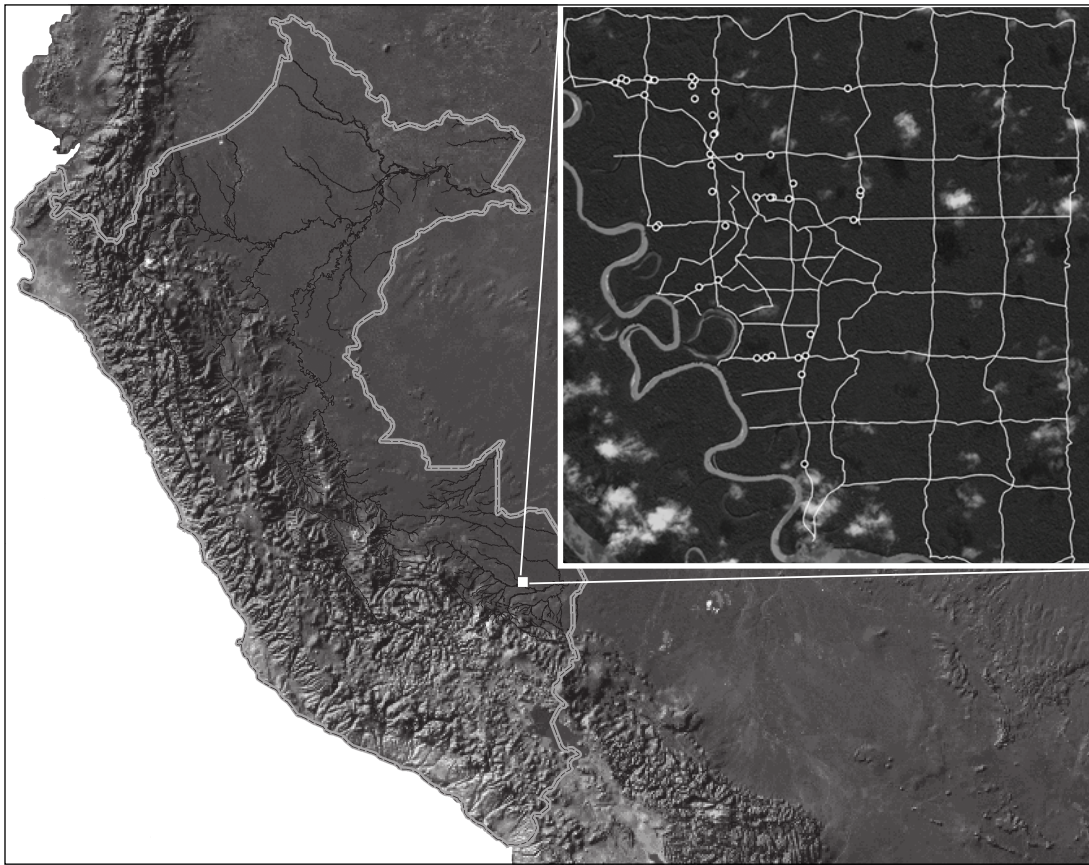


Figure 1: Location of study area in Peru, with inset showing trail system and trees used in the study, superimposed on QuickBird satellite image.

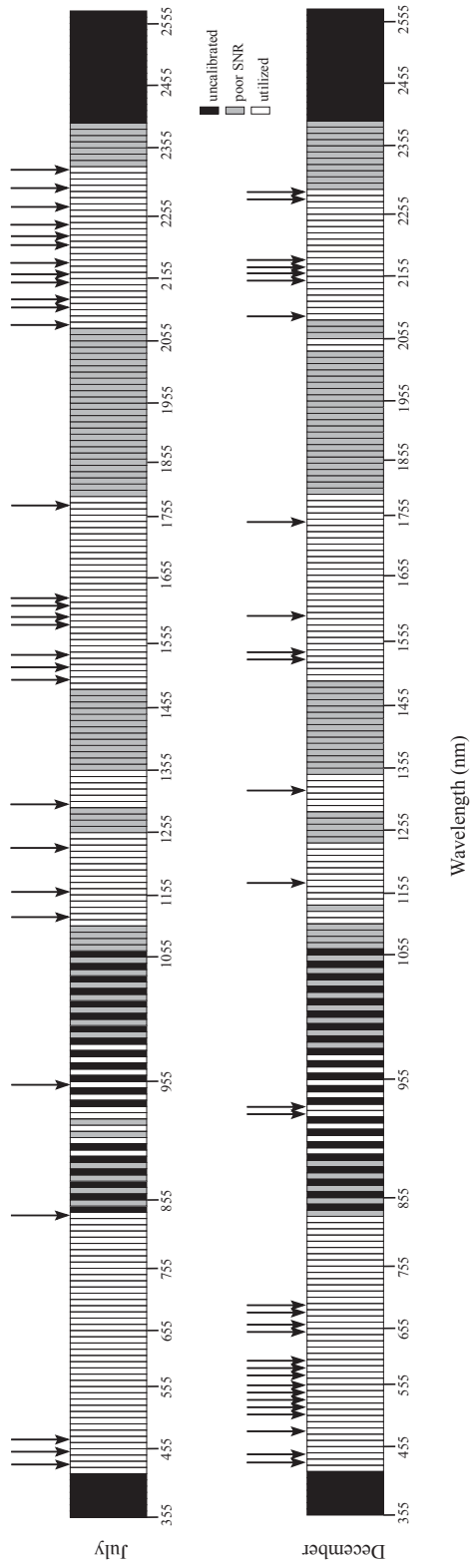


Figure 2: Hyperion hyperspectral bands from July and December 2006 images. Arrows point to bands selected with the discriminant stepwise procedure

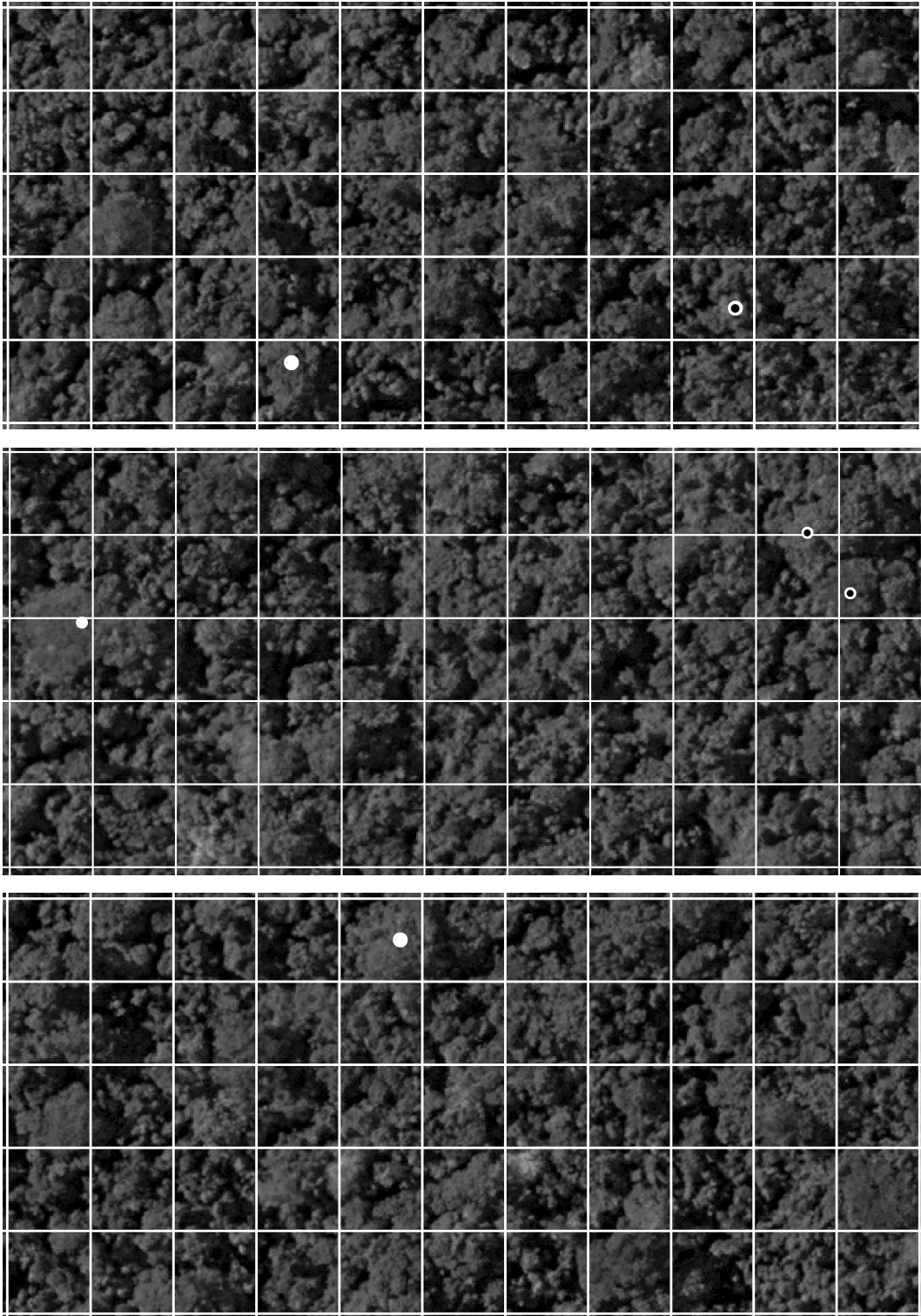


Figure 3: Example tree crowns used in the raw (black dots over white circles) and clean dataset (white circles). Hyperion spatial resolution (30 m) shown as white grid cells.

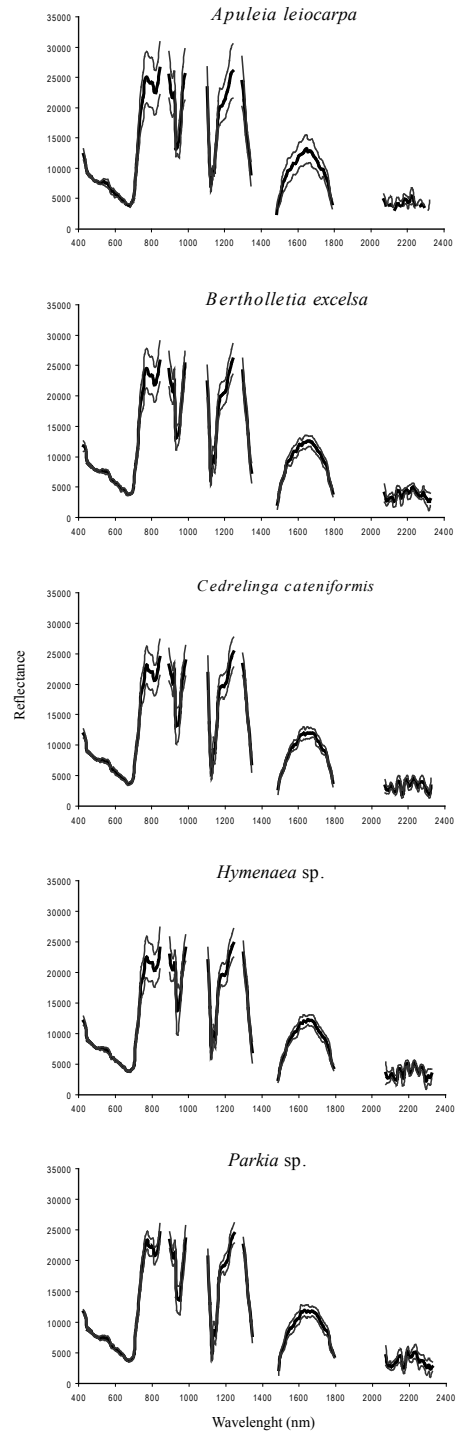
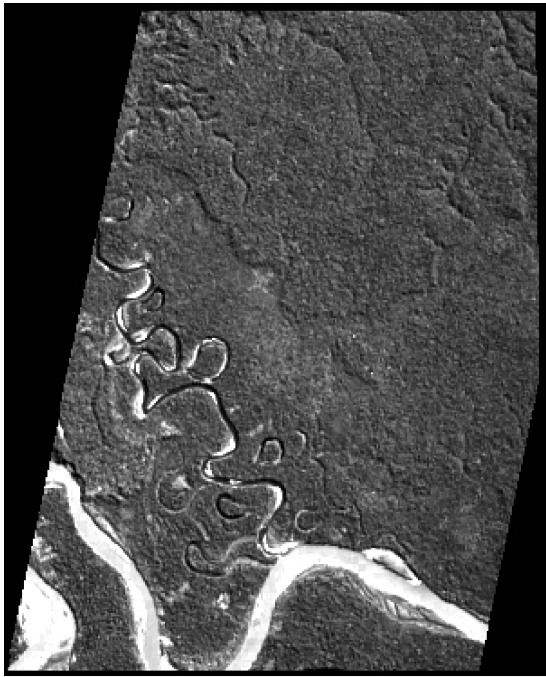


Figure 4: Hyperion 710 nm channel from July, geographic extent reduced to study area; graphs represent species mean spectra \pm 1 standard deviation extracted from July dataset containing 130 channels; gaps represent uncalibrated or noisy channels not included in the analysis.

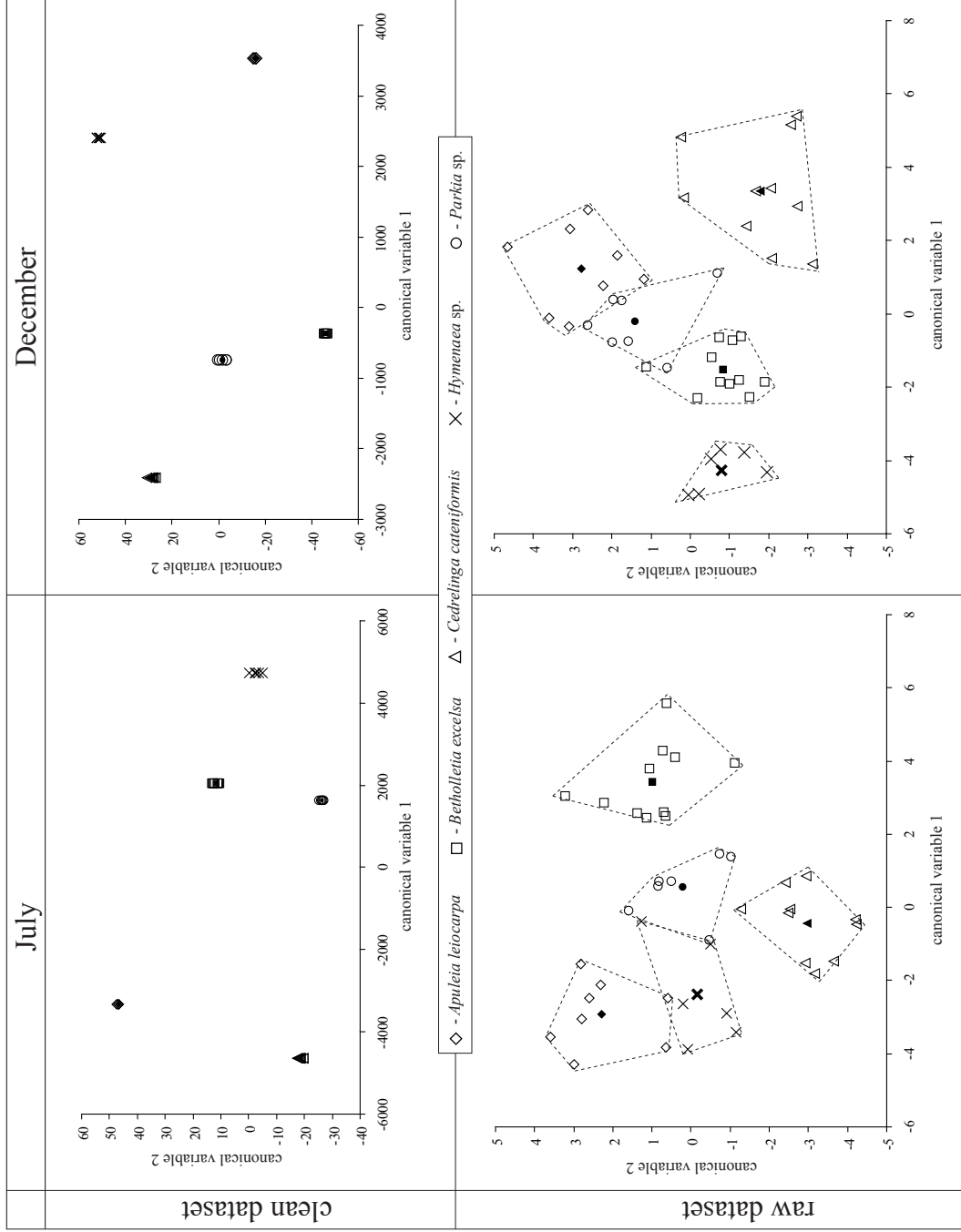


Figure 5: Position of individual tree crown spectra in canonical variable space.

CHAPTER III

Seasonal Variation in Species-Specific Spectral Signatures of Rainforest Trees in Southeastern Peru

Understanding the function and spatial distribution of ecosystems across broad extents is necessary for addressing complex urgent issues like climate change, carbon budgets, and biodiversity conservation. Detailed field-based measurements are time-consuming, limited in spatial and temporal coverage, localized spatially, and logistically and financially difficult to replicate at large scales. Such challenges are particularly notable in the tropical ecosystems, which are frequently hyperdiverse.

These challenges are being addressed via remote sensing (from air or space) of natural surfaces based on the spectral characteristics of their absorption, reflectance, and scatter of solar energy (Ustin et al. 2004). Vegetation studies in the 400-2500 nm region of the electromagnetic spectrum of reflected light have shown that the visible range (400-700 nm) is characterized by strong pigment absorption (chlorophyll, carotene, and anthocyanin); the near-infrared range (700-1300 nm) is dominated by scattering, the major biochemical contributor being water, and to a smaller degree lignin and cellulose; and the shortwave infrared range (1300-2500 nm) is characterized by low reflectance and high absorption of light by water and

vegetation components such as starch, cellulose, lignin, and nitrogen (Asner 1998; Blackburn 2002; Curran 1989).

This fundamental knowledge of vegetation spectral manifestation forms the basis of imaging spectroscopy (or hyperspectral imagery), which harvests reflected light in hundreds of narrow spectral bands (Goetz et al. 1985). These information-rich datasets have been used to study tropical ecosystem function (Asner and Vitousek 2005; forest canopy chemistry, Martin and Aber 1997) and structure (tree species richness and identification, Asner et al. 2008; Carlson et al. 2007; Clark et al. 2005; Held et al. 2003; Kalacska et al. 2007; Zhang et al. 2006). Important findings emerging from this body of research include the ideas that (1) hyperspectral imagery can be informative regarding biochemical processes and for species composition; (2) measurements of spectra at the scale of individual leaves cannot be translated directly to canopy-scale extents owing due to atmospheric effects and tree crown structural elements (e.g., bark, variable crown cover, epiphytes, etc.) influencing signals; and (3) within-species variation exists. Thanks to the latter point, although species' spectra are not unique, this variation is of lower magnitude than between-species variation. Although canopy-level spectral variation may be informative, temporal variation at this scale may influence studies of ecosystem processes and mapping tree species.

Given the difficulties of obtaining hyperspectral imagery that has adequate temporal and spatial resolution, spectral variation of species has been studied mainly at the leaf level, with on-site reflectance measurements (Castro-Esau et al. 2006;

Cochrane 2000). At the canopy level, narrow-band vegetation indices calculated from time series imaging spectroscopy have been used to compare biochemical and physiological changes of invasive and native tree species in Hawaii (Asner et al. 2006). More study has focused on time-series analysis of broad-band vegetation indices (e.g., Normalized Difference Vegetation Index, NDVI; Huete et al. 1994) derived from easily accessible multispectral, satellite imagery like the Moderate Resolution Imaging Spectroradiometer (MODIS, Justice et al. 1998). Given the coarse spectral resolution of these data (19 channels for 400 – 2500 nm range), however, only few vegetation indices can be derived, which are mostly limited to describing broad changes in forest canopy coverage, canopy water content, and photosynthetic activity (Houborg et al. 2007; Huete et al. 2008; Xiao et al. 2006; Zhang et al. 2003). These studies are important in that they describe regional seasonal phenological patterns, albeit irrespective of tree species.

In this study, we use Hyperion hyperspectral satellite imagery (Ungar et al. 2003) to examine spectra of five tropical tree taxa, and to analyze their variation at four points in time over 2006-2008. The location of the study site in hyperdiverse southeastern Peru (Foster 1993) makes the study still more challenging, both in terms of sample sizes of trees and availability of cloud-free imagery. However, as our aim is to improve understanding of tree spectral seasonality at the crown level, this analysis represents at least a first step towards achieving this aim. We use only image-derived tree canopy spectra to study temporal spectral variation, avoiding the issues of scaling up leaf spectra to canopy level; however, instead, we must take into account issues

regarding quality of hyperspectral satellite imagery, such as signal-to-noise ratio, striping, and atmospheric water absorption that can mask vegetation absorption features.

1. Methods

1.1. Study site and tree samples

Trees belonging to five taxa identified as food resources for macaws and peccaries (as part of a related study of animal foraging ecology) were mapped in tropical lowland evergreen forests along the Río Los Amigos, a tributary of the Río Madre de Dios, in southeastern Peru. The area is part of a conservation concession managed by Asociación para la Conservación de la Cuenca Amazónica (ACCA). Rainfall at this site is seasonal, being lowest in June-September (Osher and Buol 1998). Because of lack of precision in species-level identifications, two tree taxa were examined at the level of genus (Table 1). Locations of trees were recorded with GPS units, and checked on a panchromatic QuickBird satellite image with a spatial resolution of 61 cm, acquired on 24 June 2006. Because not all crowns were ≥ 30 m in diameter, we subsampled the initial, “raw” set of 42 trees to a “clean” subset of 28 trees (Table 1), all with crowns covering $\geq 40\%$ of the 30 x 30 m pixel in the Hyperion imagery (see below). In this analysis, the raw dataset was used only in preliminary analyses of species’ spectral separation to check for effects of mixed pixel signals.

1.2. Hyperspectral satellite imagery

Currently only a single satellite-based source of hyperspectral imagery is available, Hyperion, which provides data at 30 m spatial resolution. Out of a total of 30 attempts, we obtained four images of the study area, acquired on 20 July 2006 (dry season), 29 December 2006 (wet season), 19 November 2007 (beginning of wet season), and 21 May 2008 (end of wet season). We will refer to these four different “snapshots” in time as t_1 , t_2 , t_3 , and t_4 .

Un-georeferenced original radiance datasets were atmospherically corrected to apparent surface reflectance using the ACORN-6 atmospheric correction model (ImSpec, Palmdale, CA). To reduce atmospheric correction modeling errors around water absorption channels (940 and 1140 nm), a cubic spline curve was fit to these 2 narrow band regions in each pixel. Intermittent pixels with lower values create striping in some Hyperion narrow bands (Goodenough et al. 2003). This effect was corrected using a destriping algorithm that applied minor corrections (coefficients close to 1.0) on a band-by-band basis (Asner and Heidebrecht 2003). The sensor collects data across the electromagnetic spectrum in the 400-2500 nm range, in 242 separate bands. However, because 42 channels were uncalibrated and others had low signal-to-noise ratios, we retained for analysis only 126 narrow bands from each of the four temporal datasets (Fig.1).

Finally, we georeferenced Hyperion images to the QuickBird image in Geomatica 10.0 (PCI Geomatics Enterprises, Inc, Richmond Hill, ON, Canada), in the OrthoEngine module, using an “inverse rubber sheeting” procedure (Dyk et al. 2002): Hyperion images were fit to a vector file containing contours of oxbow lakes

derived from the high spatial resolution image (QuickBird). The final root mean square error (RMS) was ≤ 0.5 pixel for all four images. The crown spectral measurements for all 42 trees were extracted from these datasets in ENVI 4.5 (ITT Visual Solutions, Boulder, CO).

1.3. Statistical analyses

A. Tree crown spectral separation

The four datasets corresponding to different times of the year and different years were each analyzed separately. In each case, we ran stepwise discriminant function analysis using PROC STEPWISE in SAS (SAS Institute Inc., Cary, NC, USA) to identify the subset of the 126 bands that produced the best discriminatory model, as measured by Wilk's lambda (Huberty 1994). This approach has been used previously in remote sensing to classify tree species (Clark et al. 2005; Rivard et al. 2008), offering a convenient means by which to reduce the high dimensionality of hyperspectral imagery and correlations between channels.

The subset of bands was then used in a linear discriminant analysis that seeks the highest ratio of between-groups sums of squares to within-group sums of squares (Warner 2007) to allow classification of individual trees as to species and genera. To assess the degree to which the model predicts group memberships better than random, the Wilk's lambda, Pillai's trace, and Roy's greatest root test multivariate statistics were used in PROC DISCRIM in SAS (SAS Institute Inc., Cary, NC, USA). Raw and clean tree datasets were analyzed separately, with spectra extracted from each of the

four images. We also pooled spectra of the clean datasets across the four data sets to test whether discriminatory power is time-independent. We tested classification results via cross-validations, omitting each tree crown sequentially, and testing the predictive power of the linear discriminant analysis on the missing crown. Canonical transformation of the original variables (narrow spectral bands) allowed for visualization and comparison of spectral separation of species through time (see below).

B. Temporal variation of species' spectra

Before investigating significance of tree spectral variability between time periods, we took a random sample of forest pixels across the entire image to assess general seasonal variation in spectra. We tested the ability of linear discriminant analysis to classify pixels as to the correct time of image collection. This preliminary analysis was intended to provide information regarding general, non-species specific, vegetation spectral variation across $t_1 - t_4$.

Temporal variation of spectral characteristics of the five taxa studied was assessed using two different approaches: one based on each taxon's location in canonical spectral-dimensional space, and one based on aggregating spectral subsets obtained via stepwise discriminant function analysis and testing for reflectance differences by species and time. Variation in location of taxa in canonical space was assessed through analysis of changes in measured distances among taxa means, and an analysis of geometric differences in positions of the means.

For the first analysis, we calculated Euclidean distances among mean spectral signatures for all taxa in a two-dimensional canonical space (first and second derived canonical variables) as derived in the independent analyses described above. Canonical axes were scaled to the same values between the four independent image datasets. We thus generated four distance matrices, one for each of the t_1 , t_2 , t_3 , and t_4 datasets. To test for rearrangements in the spatial arrangement of species' centroids across the four datasets, we used a Mantel test (Mantel 1967), a randomization technique that compares sets of distance matrices for similar structure. The null hypothesis tested in this pairwise approach is that of no relationship between the matrices. In the original implementation of this test (Mantel 1967), products of corresponding elements of the matrices were summed and the observed Z statistic is compared to values obtained when the rows of one matrix are shuffled at random. A more widely used implementation computes Pearson's correlation coefficients between corresponding elements of the matrices (Legendre 2000). We calculated pairwise comparisons of matrices corresponding to t_1 - t_2 , t_2 - t_3 , and t_3 - t_4 , and used 1000 random permutations in each test. These tests were carried out in R (R Development Core Team 2008), using a package of R functions for vegetation ecologists (Oksanen et al. 2008)

Second, we tested the significance of relative positional change of taxon means in two-dimensional canonical space between the four datasets via a method adapted from the field of geometric morphometrics (Adams et al. 2004). Taxonomists have developed techniques for studying individual shape variation and delineation of

morphological characters, by digitizing such characters and their specific landmarks. These methods seek statistically significant morphological differences between individuals, and groups them based on these differences. We used the positions of the means of the taxa in the four datasets in canonical space as analogs of the landmarks. We calculated relative warps to summarize variation among data sets, with respect to an average shape obtained after fitting least squares of one configuration to another on complex regression functions (Rohlf 1993). This analysis is in fact a principal component analysis of the covariance matrix of the partial warp scores, which are computed when the shape of one individual's landmarks are projected on the average shape. We used freeware available from Stony Brook Morphometrics group (<http://life.bio.sunysb.edu/morph/index.html>): tpsTDig to digitize "landmarks" (taxon means in two-dimensional canonical space), and tpsRelW to calculate relative warps of datasets. In other words, we tested whether relative locations of taxon means change significantly between datasets: significant change would imply that variation exists in the geometric arrangement of species spectra in canonical space across time.

Finally, a multivariate analysis of variance in spectral space was carried out across the four datasets. The challenge in this case was to reconcile the four band subsets that had been selected independently for each seasonal analysis (see above) to optimize species classification. We averaged selected narrow bands into 9 broad bands that are effectively multispectral in nature (Fig.1): three in the visible range, one in the near-infrared, and five in the shortwave infrared region of the spectrum. This multispectral dataset lost the specificity and information richness of the original

narrow-band datasets, but allowed for temporal analysis of spectral variation within taxa. As such, the dataset generated for this analysis contained the average reflectance in the nine multispectral bands for the 28 trees, grouped by time period. We used a repeated measures Multivariate Analysis of Variance (MANOVA; Cole and Grizzle 1966) to test the null hypotheses (1) that variation in spectral reflectance is not taxon-specific, and (2) that time period does not affect changes in the reflectance.

Significance was tested using PROC GLM in SAS (SAS Institute Inc., Cary, NC, USA) which calculates four multivariate tests: Wilks' lambda, Pillai's trace, Hotelling-Lawley trace, and Roy's greatest root

2. Results

2.1. Tree crown spectral separation

When the clean dataset was used, the stepwise linear discriminant analysis selected 25-27 narrow bands with most discriminatory power (Fig. 1) for each temporal dataset; the raw dataset produced very different results: for t_1 and t_2 , 10-11 bands were selected, while for t_3 and t_4 0-2 bands were selected. By doubling the default significance level ($\alpha = 0.15$) for a variable to enter the raw-data model, we obtained 40-41 narrow bands selections for t_3 and t_4 , but these datasets did not perform well in discriminant analyses, with multivariate statistical tests marginally significant and large errors in cross-validation tests (Table 1). In contrast, discriminant analyses based on the clean dataset yielded statistically significant models (all $P < 0.0001$ for Wilk's lambda, $P < 0.02$ for Pillai's trace, and $P < 0.0001$ for Roy's greatest root) and

the cross-validation tests returned zero or low classification errors (Table 1). The least successful classification observed was for *Hymenaea* sp., the taxon for which sample sizes were lowest (only 4 individuals in the clean dataset). Similarly, in canonical space, individual trees did not group well by taxon when the raw dataset was used, except for spectra extracted from the t_3 dataset; in contrast, for the clean dataset, taxon classes were well-defined in canonical space (Fig.2).

The clean dataset spectra extracted from the four temporal images were also analyzed in a combined dataset. The stepwise procedure identified 30 spectral bands (Fig. 1), but these data produced large classification errors in terms of taxa in the linear discriminant analysis (Table 1); rather, these analysis identified group membership by time period (Fig.3). It appears that temporal variation is much greater than taxonomic variation. Within time periods, however, spectral separation of the tree taxa was clear and highly significant, as in our previous analyses (Papeş et al. in review).

2.2. Temporal variation of tree crown spectra

Linear discriminant analysis of the random sample of forest pixels was highly successful in classifying pixels as to temporal dataset. The largest error based on cross-validation tests was observed for t_2 (0.0022); the multivariate tests of the linear discriminant model (Wilk's lambda, Pillai's trace, and Roy's greatest root) were statistically significant (all $P < 0.0001$). This result can be interpreted as evidence for

significant overall temporal signal in the Hyperion measurements of vegetation spectral properties.

We next tested for similarity in the geometric positions of species' means in canonical space among seasons. Estimates based on Euclidean distances among means with Mantel test comparisons yielded no significant relationship between any pair of distance matrices (t_1-t_2 , t_2-t_3 , t_3-t_4 ; all $P > 0.2$), which indicates that no significant (nonrandom) similarity could be detected in positions of taxon means among time periods. Simple Mantel tests have been shown to be robust even with small or skewed samples, and to avoid type I error (rejecting the null hypothesis when it is actually true) consistently through permutation tests (Legendre 2000). The likelihood of committing type I errors of course increases when >2 pairwise comparisons are made through partial Mantel tests (Legendre 2000; Raufaste and Rousset 2002).

The relative warps analysis adapted from geometric morphometrics provided further support for the hypothesis of temporal reassortment of variation of spectral characteristics of tree species. Positions of taxon means in two-dimensional canonical space were significantly different between the temporal datasets. Indeed, we found no overlap between the shapes in principal components plots (Fig. 4).

Finally, the MANOVA of the multispectral dataset confirmed the significance of interactions between time and variation in crown spectra ($P < 0.0001$), but did not find a significant effect of taxon on observed spectral variation ($P > 0.1$). This result is not surprising, given that crown spectra were averaged over numerous (73) narrow

bands (Fig. 1), with little overlap with the narrow bands identified as informative for taxon classification when data were analyzed separately; the reduced overlap being the effect of applying a lax selection criterion of any band present in one of the four linear discriminant analysis datasets. Our expectation for the potential of repeated measures MANOVA to find significant interaction between taxa and spectral variation was low due to lack of specificity of the broad band dataset. Nevertheless, even this rather coarse spectral dataset again emphasized temporal variation in tree crown spectra.

3. Discussion

Variation through time in tree species' spectral characteristics is an important issue because it is conceivable that present and near-future technological advances in imaging spectroscopy can provide information on which to base a regional view of species' distributions and ecosystem structure and function (Chambers et al. 2007). It is thus important to understand the details of these measurements that may influence ways and the scopes for which these technologies are employed. One of these details is the focus of the present study.

We investigated spectral variability of tree crowns using hyperspectral data acquired at four different times over a two-year period. Classification of individual trees to taxon showed low or no error within each of the temporal datasets, indicating that spectral separation is possible, as had been the conclusion of our previous, simpler analyses (Papeş et al. in review). However, pooling data across time in a

single time-and taxon analysis masked the taxon signal, probably owing to more dramatic seasonal effects and possible season by taxon interactions (Fig.3).

In fact, simple visualizations of tree spectra (Fig.5) calls attention to within-species variation between the four temporal datasets. Some of the drops in reflectance that are observed are related to water absorption, particularly around 970, 1140, and 1900 nm. As such, it can be difficult to separate the relative contributions of atmospheric water vapor *versus* vegetation characteristics in producing these features. These features are most distinct in the wet (December) and dry (July) seasons. Nevertheless, since the narrow bands used in the statistical tests did not overlap with these particular regions of the spectrum, we are confident that the statistical significantly variation observed among measurements of individual tree crown spectra result from physiological and/or structural changes that occur at different times of the year. In addition, phenology monitoring in the field of most of the trees analyzed here indicates differences in the crown stages (flowering, fruiting, new leaves) between dry and wet seasons.

Our crown-level level, satellite hyperspectral approach to study spectral variation differs from previous studies addressing--to a certain degree--similar questions. In general, previous focus has been on quantifying intraspecific variation in leaf spectra, usually involving measurements of leaf spectra with hand-held or laboratory spectrometers (Castro-Esau and Kalacska 2008; Castro-Esau et al. 2006; Cochrane 2000; Rivard et al. 2008). These studies provide information necessary to evaluate the possible utility of spectra in species identification and mapping. Another

field of study that has seen considerable attention is that of temporal variation in vegetation indices. Hyperspectral datasets can be used to calculate narrow-band vegetation indices that are sufficiently specific to identify changes in pigment concentration, photosynthetic activity, leaf area, or crown cover (Asner et al. 2006; Kalacska et al. 2005).

The main scope of this study was to investigate spectral variation in a few target trees identified as important food sources for macaws and peccaries. Such information is necessary for building a future, regional-scale understanding of influences of habitat requirements and phenology in shaping animal species distribution that will aid conservation planning in the Peruvian Amazon.

REFERENCES:

- Adams, D.C., Rohlf, F.J., & Slice, D.E. (2004). Geometric morphometrics: Ten years of progress following the 'revolution'. *Italian Journal of Zoology*, 71, 5-16
- Asner, G.P. (1998). Biophysical and biochemical sources of variability in canopy reflectance. *Remote Sensing of Environment*, 64, 234-253
- Asner, G.P., & Heidebrecht, K.B. (2003). Imaging spectroscopy for desertification studies: Comparing AVIRIS and EO-1 Hyperion in Argentina drylands. *IEEE Transactions on Geoscience and Remote Sensing*, 41, 1283-1296
- Asner, G.P., Hughes, R.F., Vitousek, P.M., Knapp, D.E., Kennedy-Bowdoin, T., Boardman, J., Martin, R.E., Eastwood, M., & Green, R.O. (2008). Invasive plants transform the three-dimensional structure of rain forests. *Proceedings of the National Academy of Sciences of the USA*, 105, 4519-4523
- Asner, G.P., Martin, R.E., Carlson, K.M., Rascher, U., & Vitousek, P.M. (2006). Vegetation-climate interactions among native and invasive species in Hawaiian rainforest. *Ecosystems*, 9, 1106-1117
- Asner, G.P., & Vitousek, P.M. (2005). Remote analysis of biological invasion and biogeochemical change. *Proceedings of the National Academy of Sciences USA*, 102, 4383-4386
- Blackburn, G.A. (2002). Remote sensing of forest pigments using airborne imaging spectrometer and LIDAR imagery. *Remote Sensing of Environment*, 82, 311-321

- Carlson, K.M., Asner, G.P., Hughes, R.F., Ostertag, R., & Martin, R.E. (2007). Hyperspectral remote sensing of canopy biodiversity in Hawaiian lowland rainforests. *Ecosystems*, *10*, 536-549
- Castro-Esau, C., & Kalacska, M. (2008). Tropical dry forest phenology and discrimination of tropical tree species using hyperspectral data. In M. Kalacska & G.A. Sánchez-Azofeifa (Eds.), *Hyperspectral remote sensing of tropical and subtropical forests*. Boca Raton, FL: CRC Press
- Castro-Esau, K.L., Sánchez-Azofeifa, G.A., Rivard, B., Wright, S.J., & Quesada, M. (2006). Variability in leaf optical properties of Mesoamerican trees and the potential for species classification. *American Journal of Botany*, *93*, 517-530
- Chambers, J.Q., Asner, G.P., Morton, D.G., Anderson, L.O., Saatchi, S.S., Espírito-Santo, F.D.B., Palace, M., & Souza Jr, C. (2007). Regional ecosystem structure and function: Ecological insights from remote sensing of tropical forests. *Trends in Ecology and Evolution*, *22*, 414-423
- Clark, M.L., Roberts, D.A., & Clark, D.B. (2005). Hyperspectral discrimination of tropical rain forest tree species at leaf to crown scales. *Remote Sensing of Environment*, *96*, 375-398
- Cochrane, M.A. (2000). Using vegetation reflectance variability for species level classification of hyperspectral data. *International Journal of Remote Sensing*, *21*, 2075-2087
- Cole, J.W.L., & Grizzle, J.E. (1966). Applications of Multivariate Analysis of Variance to repeated measurements experiments. *Biometrics*, *22*, 810-828

- Curran, P.J. (1989). Remote sensing of foliar chemistry. *Remote Sensing of Environment*, 30, 271-278
- Dyk, A., Goodenough, D.G., Bhogal, A.S., Pearlman, J., & Love, J. (2002). Geometric correction and validation of Hyperion and ALI data for EVEOSD. *Proceedings of the IEEE International Geoscience and Remote Sensing Symposium (IGARSS '02), Toronto (Ontario), Canada, Vol. 1.* (pp. 579-583).
- Foster, R.B. (1993). The floristic composition of the Rio Manu floodplain forest. In A.H. Gentry (Ed.), *Four Neotropical rainforests* (pp. 99-379). New Haven, NY: Yale University Press
- Goetz, A.F.H., Vane, G., Solomon, J.E., & Rock, B.N. (1985). Imaging spectrometry for Earth remote sensing. *Science*, 228, 1147-1153
- Goodenough, D.G., Dyk, A., Niemann, K.O., Pearlman, J.S., Hao, C., Han, T., Murdoch, M., & West, C. (2003). Processing Hyperion and ALI for forest classification. *IEEE Transactions on Geoscience and Remote Sensing*, 41, 1321-1331
- Held, A., Ticehurst, C., Lymburner, L., & Williams, N. (2003). High resolution mapping of tropical mangrove ecosystems using hyperspectral and radar remote sensing. *International Journal of Remote Sensing*, 24, 2739-2759
- Houborg, R., Soegaard, H., & Boegh, E. (2007). Combining vegetation index and model inversion methods for the extraction of key vegetation biophysical parameters using Terra and Aqua MODIS reflectance data. *Remote Sensing of Environment*, 106, 39-58

- Huberty, C. (1994). *Applied discriminant analysis*. New York, NY: Wiley-Interscience
- Huete, A., Justice, C., & Liu, H. (1994). Development of vegetation and soil indexes for MODIS-EOS. *Remote Sensing of Environment*, 49, 224-234
- Huete, A., Kim, Y., Ratana, P., Didan, K., Shimabukoro, Y.E., & Miura, T. (2008). Assessment of phenologic variability in Amazon tropical rainforests using hyperspectral Hyperion and MODIS satellite data. In M. Kalacska & G.A. Sánchez-Azofeifa (Eds.), *Hyperspectral remote sensing of tropical and subtropical forests* (pp. 233-259). Boca Raton, FL: CRC Press
- Justice, C.O., Vermote, E., Townshend, J.R.G., Defries, R., Roy, D.P., Hall, D.K., Salomonson, V.V., Privette, J.L., Riggs, G., Strahler, A., Lucht, W., Myneni, R.B., Knyazikhin, Y., Running, S.W., Nemani, R.R., Wan, Z., Huete, A.R., van Leeuwen, W., Wolfe, R.E., Giglio, L., Muller, J.-P., Lewis, P., & Barnsley, M.J. (1998). The Moderate Resolution Imaging Spectroradiometer (MODIS): Land remote sensing for global change research. *IEEE Transactions in Geosciences and Remote Sensing*, 36, 1228-1249
- Kalacska, M., Sánchez-Azofeifa, G.A., Calvo-Alvarado, J., Rivard, B., & Quesada, M. (2005). Effects of season and succesional stage on Leaf Area Index and spectral vegetation indices in three Mesoamerican tropical dry forests. *Biotropica*, 37, 486-496
- Kalacska, M., Sánchez-Azofeifa, G.A., Rivard, B., Caelli, T., White, H.P., & Calvo-Alvarado, J.C. (2007). Ecological fingerprinting of ecosystem succession:

- estimating secondary tropical dry forest structure and diversity using imaging spectroscopy. *Remote Sensing of Environment*, 108, 82-96
- Legendre, P. (2000). Comparison of permutation methods for the partial correlation and partial Mantel tests. *Journal of Statistical Computation and Simulation*, 67, 37-73
- Mantel, N. (1967). Detection of disease clustering and a generalized regression approach. *Cancer Research*, 27, 209-220
- Martin, M.E., & Aber, J.D. (1997). High spectral resolution remote sensing of forest canopy lignin, nitrogen, and ecosystem processes. *Ecological Applications*, 7, 431-443
- Oksanen, J., Kindt, R., Legendre, P., O'Hara, B., Simpson, G.L., Solymos, P., Stevens, M.H.H., and Wagner, H (2008). *vegan: Community Ecology Package*. R package version 1.15-1.
- Osher, L.J., & Buol, S.W. (1998). Relationship of soil properties to parent material and landscape position in eastern Madre de Dios, Peru. *Geoderma*, 83, 143-166
- R Development Core Team (2008). *R: A language and environment for statistical computing*. R Foundation for Statistical Computing, Vienna, Austria
- Raufaste, N., & Rousset, F. (2002). Are partial Mantel tests adequate? *Evolution*, 55, 1703-1705
- Rivard, B., Sánchez-Azofeifa, G.A., Foley, S., & Calvo-Alvarado, J.C. (2008). Species classification of tropical tree leaf reflectance and dependence on

- selection of spectral bands. In M. Kalacska & G.A. Sánchez-Azofeifa (Eds.), *Hyperspectral remote sensing of tropical and subtropical forests* (pp. 141-159). Boca Raton, FL: CRC Press
- Rohlf, F.J. (1993). Relative warp analysis and an example of its application to mosquito wings. In L.F. Marcus, E. Bello & A. Garcia-Valdecasas (Eds.), *Contributions to Morphometrics*. Madrid, Spain: Museo Nacional de Ciencias Naturales (CSIC)
- Ungar, S.G., Pearlman, J.S., Mendenhall, J.A., & Reuter, D. (2003). Overview of the Earth Observing One (EO-1) mission. *IEEE Transactions on Geoscience and Remote Sensing*, *41*, 1149-1159
- Ustin, S.L., Roberts, D.A., Gamon, J.A., Asner, G.P., & Green, R.O. (2004). Using imaging spectroscopy to study ecosystem processes and properties. *BioScience*, *54*, 523-534
- Warner, R.M. (2007). *Applied statistics: From bivariate through multivariate techniques*. Thousand Oaks, CA: Sage Publications
- Xiao, X.M., Hagen, S., Zhang, Q.Y., Keller, M., & Moore, B. (2006). Detecting leaf phenology of seasonally moist tropical forests in South America with multi-temporal MODIS images. *Remote Sensing of Environment*, *103*, 465-473
- Zhang, J., Rivard, B., Sánchez-Azofeifa, A., & Castro-Esau, C. (2006). Intra- and inter-class spectral variability of tropical tree species at La Selva, Costa Rica: Implications for species identification using HYDICE imagery. *Remote Sensing of Environment*, *105*, 129-141

Zhang, X.Y., Friedl, M.A., Schaaf, C.B., Strahler, A.H., Hodges, J.C.F., Gao, F.,
Reed, B.C., & Huete, A. (2003). Monitoring vegetation phenology using
MODIS. *Remote Sensing of Environment*, 84, 471-475

Table 1: List of taxa with number of individuals and classification errors based on four hyperspectral datasets and two tree datasets, based on crown sizes (see Methods)

Dataset	Tree species	N	t₁	t₂	t₃	t₄
Clean	<i>Apuleia leiocarpa</i>	6	0	0	0	0
	<i>Bertholletia excelsa</i>	7	0	0	0	0.1429
	<i>Cedrelinga</i>	5	0	0	0	0
	<i>cateniformis</i>					
	<i>Hymenaea</i> sp.	4	0	0.25	0.25	0
	<i>Parkia</i> sp.	6	0	0	0	0
Raw	<i>Apuleia leiocarpa</i>	8	1	0.5	0.25	0.75
	<i>Bertholletia excelsa</i>	11	0.3636	0.7273	0	0.7273
	<i>Cedrelinga</i>	10	0.4	0.6	0.2	0.8
	<i>cateniformis</i>					
	<i>Hymenaea</i> sp.	6	0.5	0.8333	0	0.8333
	<i>Parkia</i> sp.	7	0.5714	0.1429	0	0.7143
Clean; t₁- t₄ combined	<i>Apuleia leiocarpa</i>	8	0.5	0.1667	0.5	0.3333
	<i>Bertholletia excelsa</i>	11	0.2857	0.7143	0.5714	0.5714
	<i>Cedrelinga</i>	10	1	0.6	0.6	1
	<i>cateniformis</i>					
	<i>Hymenaea</i> sp.	6	0.75	0.5	1	1
	<i>Parkia</i> sp.	7	0.8333	0.6667	0.8333	0.5

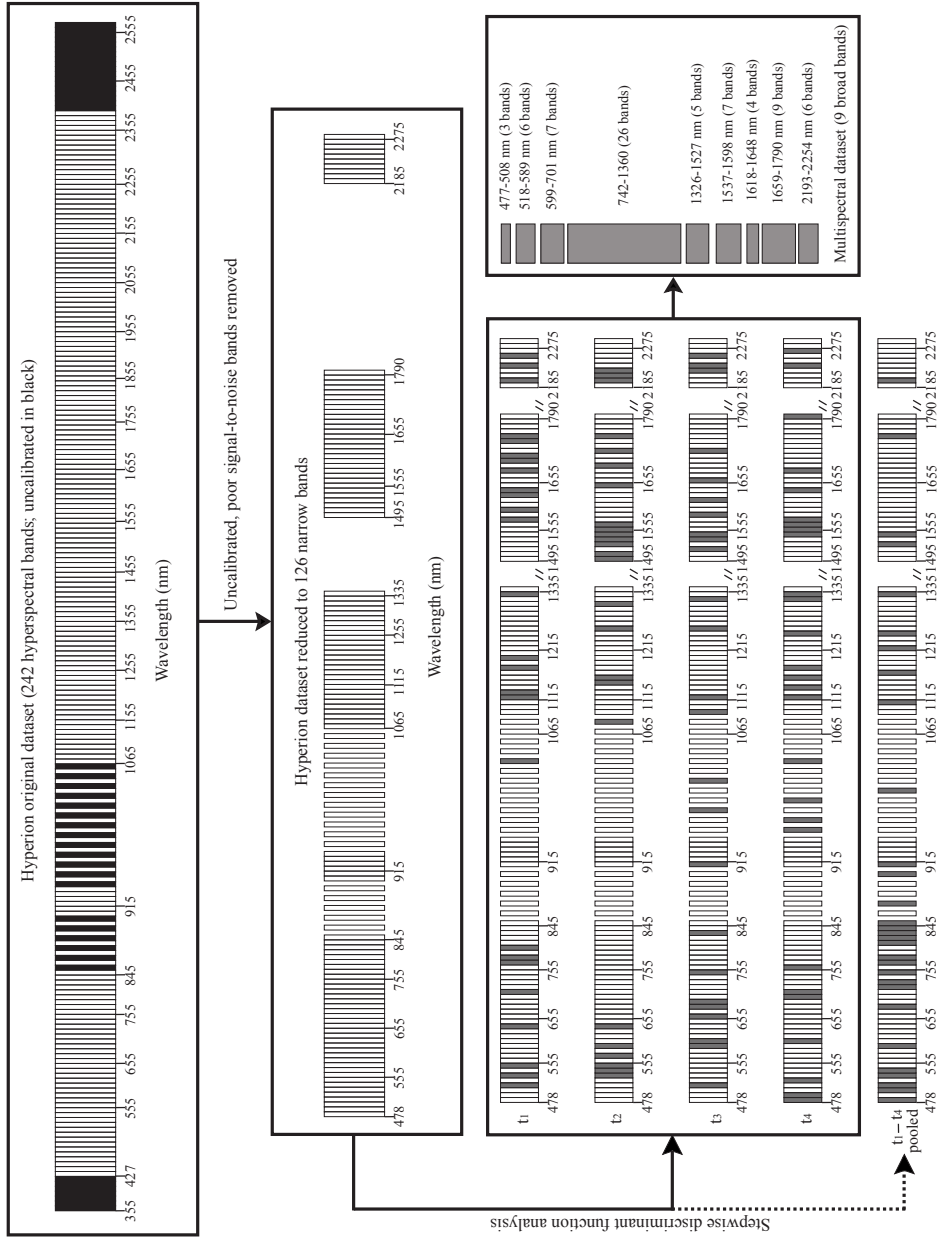


Figure 1: Summary of selection of Hyperion narrow bands for analysis. The lower left panel shows channels used in linear discriminant analyses (one analysis per image). Selection of narrow bands when $t_1 - t_4$ datasets are pooled is shown separately. The lower right panel presents the combination of channels used in the repeated measures analysis of variance (MANOVA).

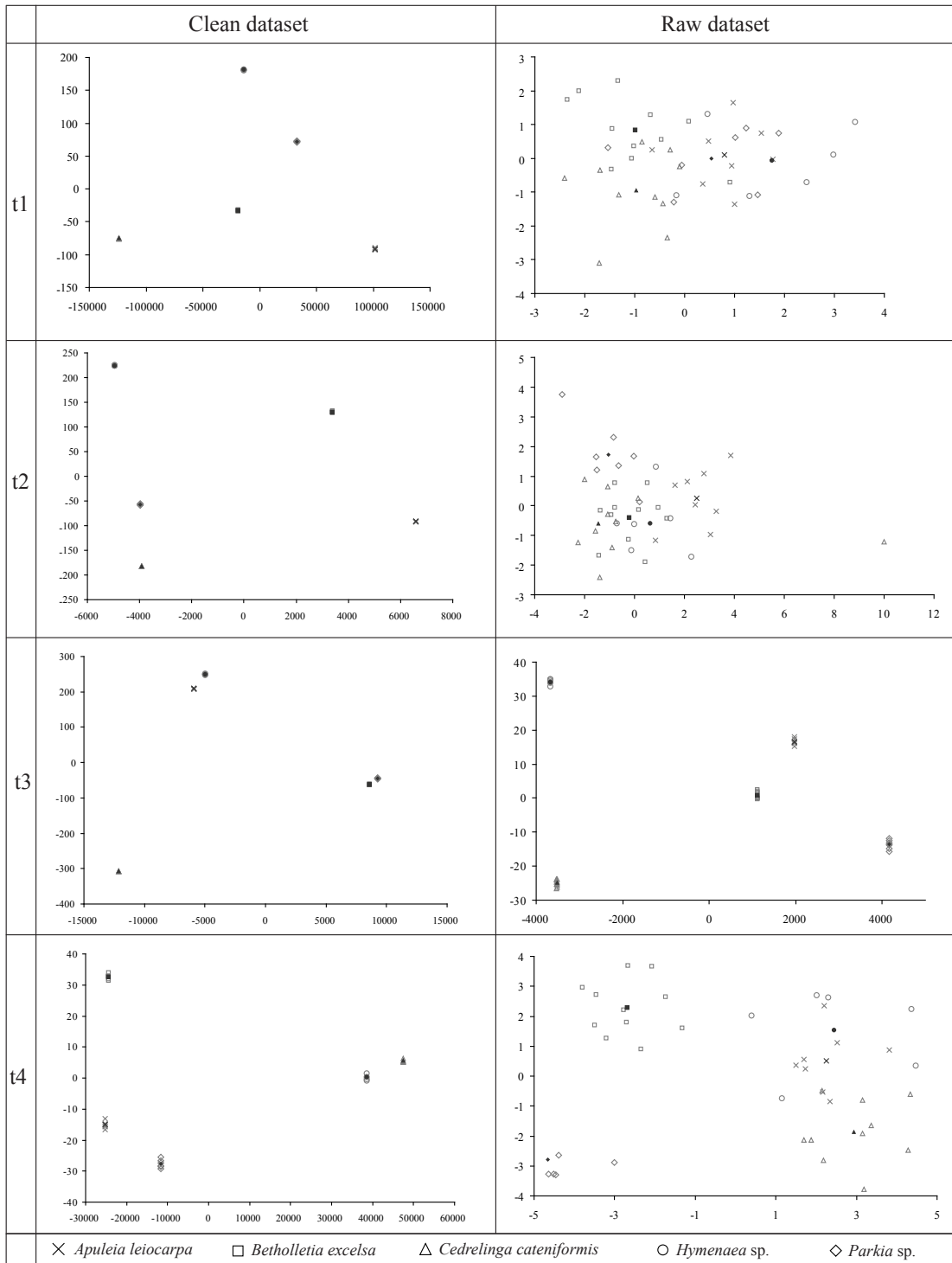


Figure 2: Representation of individual trees (lighter symbols) and taxon means (darker symbols) in canonical variable spaces generated independently for the t1 - t4 datasets.

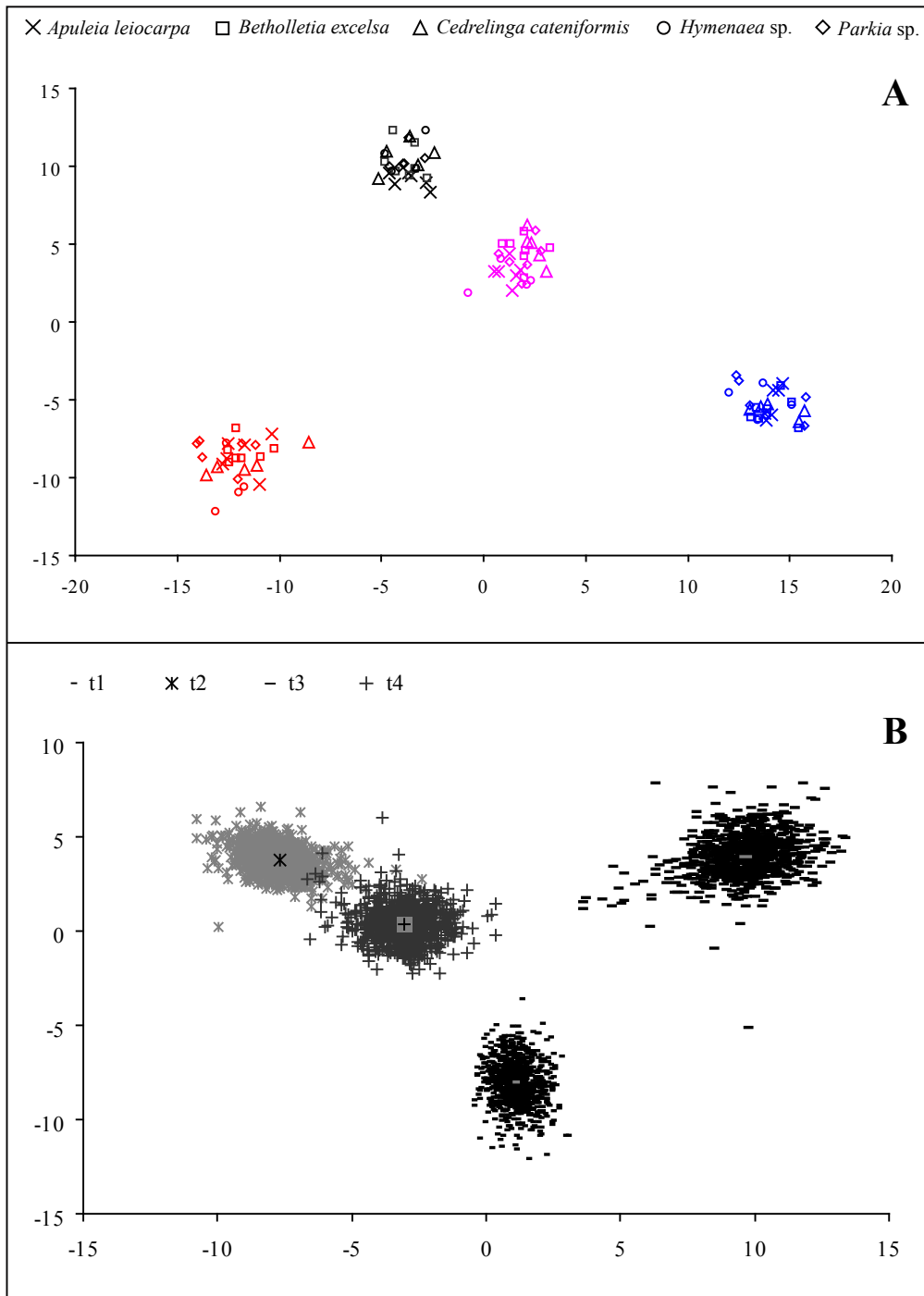


Figure 3: Temporal spectral variation observed in canonical variable space: (A) representation of t1 - t4 datasets and all (28) individual trees, showing separation through time (t1 – black, t2 – blue, t3 – red, and t4 – purple), not by taxon; (B) a random sample of pixels falling in forested areas, also grouped by time.

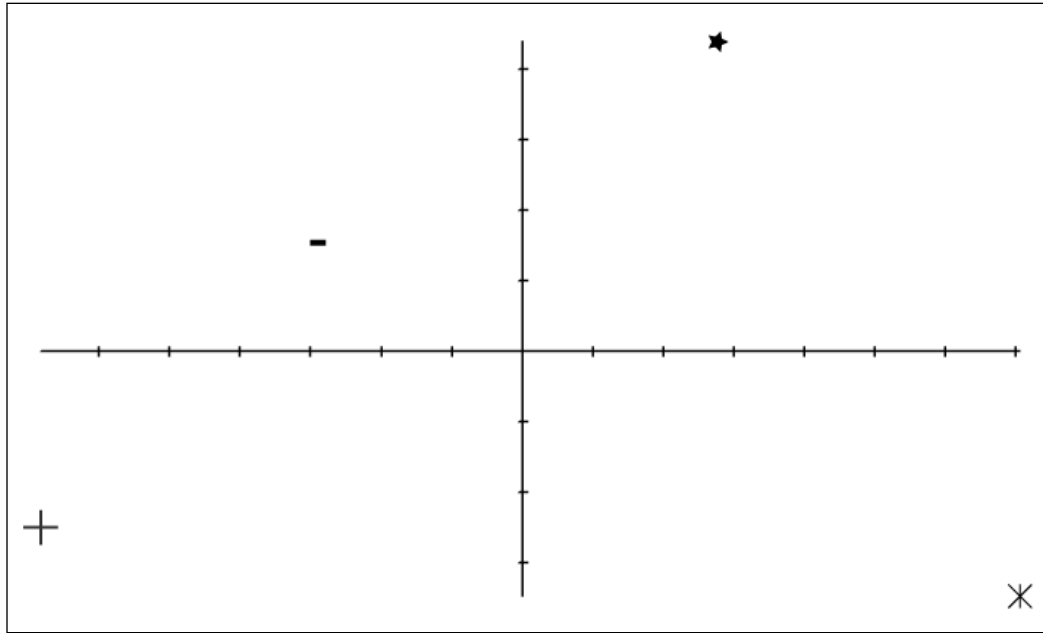


Figure 4: Differences in canonical variable space of taxa through time (t1 asterisk, t2 dash, t3 cross, t4 star), obtained with relative warps analysis.

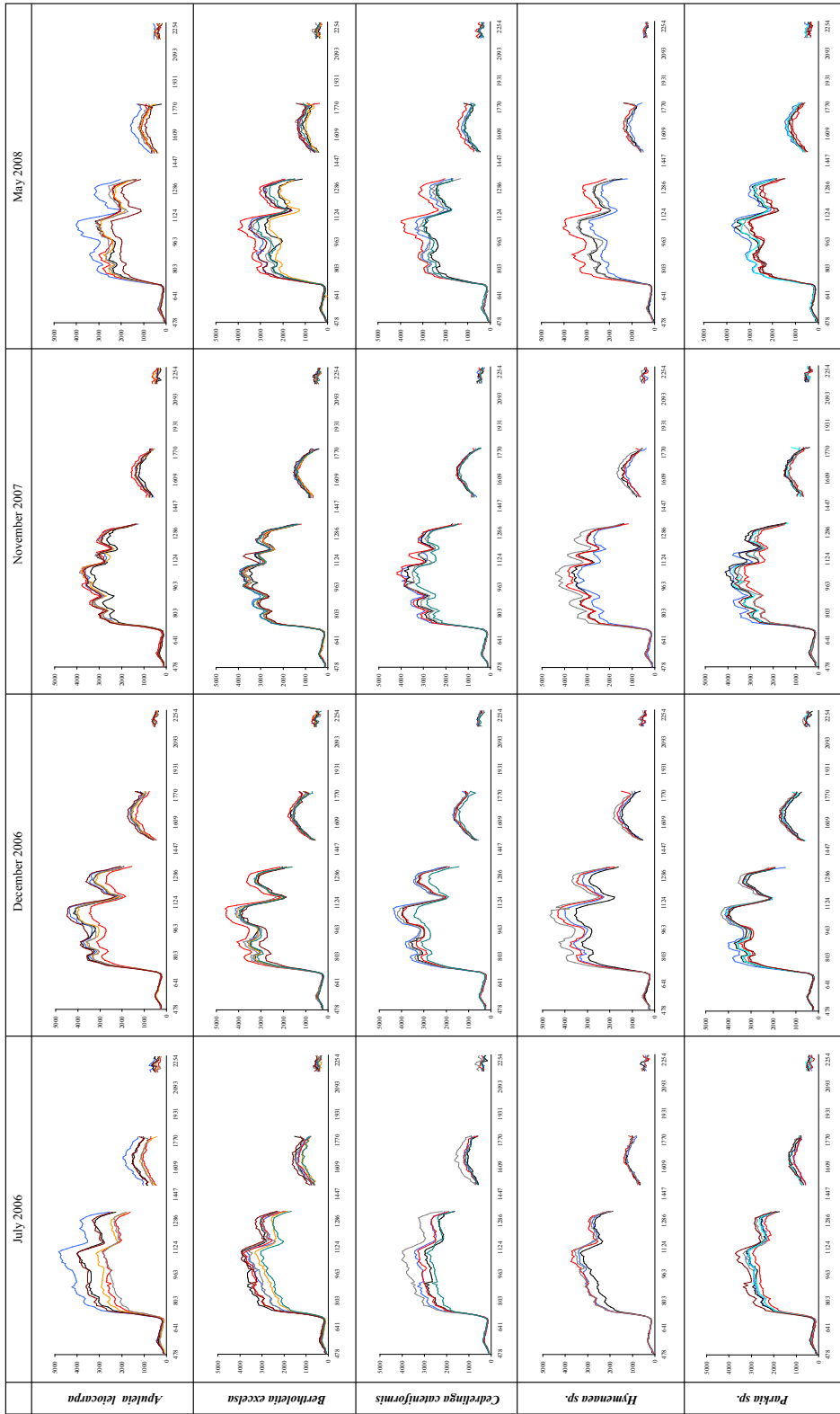


Figure 5: Spectra of tree crowns of the 5 tree taxa studied (clean dataset shown only), with uncalibrated Hyperion bands removed; colors represent different individuals of the same taxon.